RSC Advances

REVIEW

View Article Online
View Journal | View Issue

Check for updates

Cite this: *RSC Adv.*, 2026, **16**, 2555

Thermal management of lithium-ion batteries: from single cooling to hybrid cooling

Zhang Qianqian,[a] Zhang Wei,[a] Wang Siyang,[a] Yang Xufei, *[a] Liu Guanglin,[b] Sun Dongliang[a] and Yu Bo [c]

To address safety hazards from battery thermal runaway and efficiency losses caused by temperature non-uniformity, a systematic review is conducted on the evolution of thermal management technologies for lithium-ion batteries. Guided by the transition from single cooling strategies to composite systems that integrate and coordinate multiple approaches, a four-dimensional analytical framework has been established, encompassing air cooling, liquid cooling, phase-change material (PCM) cooling, and hybrid cooling technologies. Findings indicate that air-cooling systems retain a cost advantage in medium-to small-scale applications with relatively low energy density, where optimization efforts primarily focus on battery array configuration and airflow channel design. Liquid-cooling methods—such as cold-plate liquid cooling, immersion cooling, and heat-pipe cooling—have emerged as the mainstream solution in high-energy-density systems, with future research expected to address challenges related to cold-plate heat-exchange structures, fluid-distribution uniformity, and coolant selection. PCM cooling enables passive temperature regulation through the latent heat of solid–liquid phase transitions; however, its low thermal conductivity and phase-change hysteresis necessitate the synergistic application of advanced composite PCMs and enhanced heat-exchange structures. Multi-component hybrid cooling technologies, which simultaneously address temperature uniformity and rapid heat-dissipation demands under variable operating conditions such as high charge/discharge rates, are expected to become a major focus in the next stage of lithium-ion battery thermal management development.

Received 19th October 2025
Accepted 15th December 2025

DOI: 10.1039/d5ra08014b

rsc.li/rsc-advances

Open Access Article. Published on 12 January 2026. Downloaded on 4/4/2026 5:57:19 AM.
This article is licensed under a Creative Commons Attribution-NonCommercial 3.0 Unported Licence.

1. Introduction

In recent years, lithium-ion batteries have been widely deployed in electric vehicles and energy storage systems owing to their high energy density; however, the safety issues associated with thermal runaway have become increasingly prominent. Thermal runaway involves rapid temperature escalation, violent exothermic reactions, and the release of flammable gases, potentially leading to fire or explosion. These hazards underscore the critical need for effective Battery Thermal Management Systems (BTMS) to ensure safe operation in both energy storage stations and power battery applications.[1]

Among various energy storage technologies, lithium-ion battery-based electrochemical storage has become the predominant solution due to its high energy density, long cycle life, and fast response capability. Nevertheless, the rapid growth in large-scale deployment has been accompanied by rising safety concerns, particularly those associated with overheating and thermal runaway. As the energy density of lithium-ion batteries continues to rise, incidents of fire and explosion caused by thermal runaway have occurred with increasing frequency, posing significant risks to both the stability of power systems and the safety of personnel. Research indicates that the optimal operating temperature range for lithium-ion batteries is 25 °C-40 °C,[2,3] and that the maximum allowable temperature difference between cells should not exceed 5 °C.[4] However, during high-rate charging and discharging, lithium-ion battery temperatures tend to exceed the optimal range, leading to reduced temperature uniformity and accelerated degradation. Sustained exposure to elevated temperatures not only exacerbates side reactions in electrolytes and electrodes but also induces irreversible structural changes, leading to rapid performance decay. Under such conditions, the battery's internal resistance increases, accelerating the decomposition of electrolytes and electrode materials. This process generates significant quantities of combustible gases and heat, causing rapid rises in internal temperature and pressure. Ultimately, this shortens battery lifespan and, in severe cases, may trigger safety incidents such as fires and explosions.[5,6] Another critical issue lies in temperature non-uniformity within a battery pack. Variations in local heat generation and insufficient cooling pathways can cause some cells to operate at significantly higher

[a]*School of Mechanical Engineering, Beijing Institute of Petrochemical Technology, Beijing 102617, China. E-mail: yangxufei@bipt.edu.cn*

[b]*School of Energy, Power and Mechanical Engineering, North China Electric Power University, Beijing 102206, China*

[c]*School of Petroleum Engineering, Yangtze University, Wuhan 430100, China*

© 2026 The Author(s). Published by the Royal Society of Chemistry

Open Access Article. Published on 12 January 2026. Downloaded on 4/4/2026 5:57:19 AM. This article is licensed under a Creative Commons Attribution-NonCommercial 3.0 Unported Licence.

temperatures than others. This aggravates the so-called "weakest link" effect, whereby the performance and reliability of the entire energy storage station are constrained by the most vulnerable module. As a result, uneven thermal distribution significantly undermines the overall integrity, operational stability, and economic viability of energy storage projects.[7] For utility-scale systems designed for service lifetimes of 15–20 years, such uneven degradation can result in substantial maintenance costs, early retirement of battery packs, and reduced return on investment.

From an application perspective, BTMS requirements differ significantly between energy storage batteries and power batteries. Energy storage systems demand long-term thermal stability, low maintenance costs, and the ability to maintain uniform temperatures across large battery arrays. In contrast, power batteries—such as those used in electric vehicles—require rapid thermal response, high cooling capacity under transient peaks, and precise temperature control to ensure performance and safety.[8] lithium-ion battery thermal management technologies can generally be categorized into air cooling, liquid cooling, phase-change material (PCM) cooling, and coupled cooling.[9,10] Each approach possesses distinct advantages and inherent limitations, and the choice of cooling technology should be determined by a comprehensive assessment of performance, cost, complexity, and reliability. A comparison of the thermal management characteristics for several common lithium-ion battery technologies are summarized in Table 1 early energy storage projects predominantly employed air cooling, owing to its structural simplicity, ease of maintenance, and low cost. However, as battery energy density has risen, the inherent trade-off between low-cost simplicity and insufficient cooling efficiency has become more pronounced, rendering air cooling increasingly unsuitable for high-power or high-capacity systems.[11] In contrast, liquid cooling has gradually emerged as the mainstream solution for large-scale and high-energy-density applications, owing to its higher thermal conductivity and superior ability to maintain temperature uniformity.[12] Several variants have been developed, including cold-plate liquid cooling, immersion cooling, and heat-pipe-assisted liquid cooling, each addressing different operational scenarios. For instance, cold-plate systems are widely adopted in commercial applications, whereas immersion cooling shows strong potential for high-power density systems requiring ultra-fast response. PCM cooling achieves passive thermal management by exploiting the latent heat storage capacity of PCMs, thereby reducing reliance on active energy consumption and enhancing system stability.[13] It effectively suppresses peak temperature rise and enhances uniformity, though its practical application is constrained by low intrinsic thermal conductivity and interfacial resistance. To address these challenges, composite PCMs with enhanced conductivity, leakage resistance, and mechanical flexibility are actively being explored. Finally, coupled cooling systems—which integrate two or more cooling strategies such as liquid cooling, PCMs, microchannels, and thermoelectric elements—offer the potential to balance performance, energy efficiency, and system cost. This hybrid approach is increasingly recognized as a promising direction for future BTMS development.[14] The emergence of intelligent coupled systems, which combine thermal management hardware with smart control algorithms and multiphysics simulations, represents a major trend, allowing systems to dynamically adapt to diverse operating conditions.

The importance of BTMS extends beyond safety management. Efficient thermal regulation is directly linked to the reliability, service life, and economic feasibility of energy storage projects. By maintaining cells within safe operating windows, BTMS reduces degradation rates, extends cycle life, and decreases the levelized cost of storage. Moreover, advanced BTMS designs incorporating intelligent control algorithms, adaptive cooling strategies, and multi-physics optimization can dynamically adjust cooling modes according to real-time load profiles, further improving system flexibility and efficiency. These capabilities are particularly vital for next-generation energy systems that demand both high reliability and economic competitiveness.

However, existing review studies tend to focus either on a single cooling method or on general overviews of BTMS, lacking a unified comparative framework that systematically integrates multiple thermal management strategies. To address this gap, this study aims to provide a comprehensive and forward-looking review of BTMS technologies for lithium-ion energy storage systems. First, the fundamental heat-generation mechanisms of lithium-ion batteries are analyzed. Second, the working principles, performance characteristics, and application limitations of three primary cooling methods—air cooling, liquid cooling, and PCM cooling—are systematically examined. Third, the latest advancements in coupled cooling technologies are discussed, emphasizing their ability to integrate the strengths of multiple approaches. Finally, future research trends and challenges are outlined, with a focus on intelligent control, environmentally sustainable cooling media, system miniaturization, and multi-physics-field optimization. This paper holds important guiding significance for the optimization and modification of existing BTM systems, as well as the innovative design of future thermal management solutions.

2. Analysis of the heat generation mechanism in lithium-ion batteries

Lithium-ion batteries store and release electrical energy through electrochemical reactions, which fundamentally involve the migration of lithium ions between the positive and negative electrodes, thereby converting electrical energy into chemical energy (charging) or *vice versa* (discharging). Taking lithium iron phosphate ($LiFePO_4$) batteries as an example, the electrochemical reaction equations for charging and discharging are given in eqn (1)–(3):[11]

Positive-electrode reaction:

$$LiFePO_4 \Leftrightarrow Li_{1-x}FePO_4 + xLi^+ + xe^- \quad (1)$$

Negative-electrode reaction:

$$xLi^+ + xe^- + 6C \Leftrightarrow Li_xC_6 \quad (2)$$

© 2026 The Author(s). Published by the Royal Society of Chemistry

Open Access Article. Published on 12 January 2026. Downloaded on 4/4/2026 5:57:19 AM.
This article is licensed under a Creative Commons Attribution-NonCommercial 3.0 Unported Licence.

Table 1 Characteristics of common thermal management technologies for lithium-ion batteries

Future development directions	Main application scenarios	Reliability	Complexity	Cost	Main disadvantages	Main advantages	Principle	Cooling method
Optimization of duct design, airflow organization, and intelligent fan speed control	Residential energy storage and small-scale commercial energy storage systems	High	Low	Low	Limited heat dissipation efficiency, poor temperature uniformity, potential noise issues	Low cost, simple structure, easy maintenance	Utilizes natural or forced airflow, driven by fans, to pass over the battery surface or through internal channels for heat dissipation	Air cooling
Optimization of cold plate structure, flow field design, and development of novel coolants	Fixed energy storage systems with relatively high energy density	Medium	Medium–high	Medium–high	Complex piping, increased weight, leakage risk, higher maintenance cost	High heat dissipation efficiency, relatively good temperature uniformity, mature technology	Uses liquid flowing through cold plates to absorb heat, which is then released *via* heat exchangers	Cold-plate liquid cooling
Development of low-cost, safe, environmentally friendly, and long-life cooling media; system integration optimization; standardization	High-density fixed energy storage systems	Medium (depends on fluid aging)	High	High	High initial investment, fluid compatibility issues, inconvenient maintenance	Extremely high heat dissipation efficiency and temperature uniformity, low noise	Directly immerses batteries in an insulating liquid for cooling, which can operate in single-phase or two-phase modes	Immersion liquid cooling
Development of cost-effective heat pipes, optimization of battery-heat pipe integration, combination with other cooling methods	Hybrid cooling systems or applications requiring efficient passive heat transfer in space-constrained environments	High	Medium	Medium	Limited heat transfer distance, restricted applicable power range, relatively complex integration design	Very high thermal conductivity, passive operation, noiseless	Utilizes phase-change working fluid in a sealed chamber to achieve high-efficiency heat transfer through evaporation–condensation cycles	Heat-pipe liquid cooling
Improve the thermal conductivity of composite PCM, optimize encapsulation technology, a ntegration with other cooling methods	Commonly used in hybrid cooling systems or scenarios requiring high temperature uniformity	High	Low–medium	Medium	Low intrinsic thermal conductivity of materials, slow heat release, short-term regulation only, potential leakage issues	Passive operation, excellent temperature uniformity, no moving parts, compact size	Uses the latent heat of phase change materials to absorb/release heat, buffering temperature fluctuations	Solid–liquid phase change material (PCM) cooling
Optimization of coordination between different cooling technologies and development of intelligent integrated control strategies	Fixed energy storage systems with stringent thermal management requirements, where single technology is insufficient	Medium–high	High	High	Complex design, high cost, requires precise control	Customizable optimal solutions, high thermal management efficiency	Combines two or more cooling technologies to achieve complementary advantages	Coupled cooling

© 2026 The Author(s). Published by the Royal Society of Chemistry

Open Access Article. Published on 12 January 2026. Downloaded on 4/4/2026 5:57:19 AM. This article is licensed under a Creative Commons Attribution-NonCommercial 3.0 Unported Licence.

Overall reaction:

$$LiFePO_4 + 6C \Leftrightarrow Li_{1-x}FePO_4 + Li_xC_6 \quad (3)$$

During charging and discharging, heat is inevitably generated within the battery. This heat is primarily dissipated to the surrounding environment *via* thermal conduction and convection, while the remainder causes the battery temperature to rise. To quantitatively describe the battery's thermal behavior, the energy conservation is expressed as eqn (4):

$$\rho C_p \frac{\partial T}{\partial t} = \frac{\partial}{\partial x}\left(k_x \frac{\partial T}{\partial x}\right) + \frac{\partial}{\partial y}\left(k_y \frac{\partial T}{\partial y}\right) + \frac{\partial}{\partial z}\left(k_z \frac{\partial T}{\partial z}\right) + Q \quad (4)$$

where ρ is the solid density (kg m^{-3}); C_p is the specific heat capacity (J kg^{-1} K^{-1});k_x, k_y and k_z are the thermal conductivities in the *x*-, *y*-, and *z*-directions (W m^{-1} K^{-1}), respectively; and Q represents the heat source (W m^{-3}).

The total heat generated by a lithium-ion battery consists primarily of reaction heat (Q_{rev}), Joule heat (Q_{ohm}), and polarization heat (Q_{pol}),[15] as expressed in eqn (5):

$$Q_c = Q_{rev} + Q_{ohm} + Q_{pol} \quad (5)$$

Reaction heat originates mainly from electrochemical reactions occurring at the positive and negative electrodes during charging and discharging, and constitutes reversible heat, as shown in eqn (6). During charging, heat is absorbed and reaction heat is negative, whereas during discharging, heat is released and reaction heat is positive:[16]

$$Q_{rev} = a_s J_i^{Li} T\left(\frac{\partial E_{eq,i}}{\partial T}\right) \quad (6)$$

In the eqn (6), a_s is the specific interfacial area (m^2 m^{-3}), J_i^{Li}denotes the lithium-ion exchange current density, T is the thermodynamic temperature (K), and $\partial E_{eq,i}/\partial T$ is the temperature coefficient of the cell potential.

Due to internal material resistance and contact resistance, the heat generated during charging and discharging is Joule heat, which is irreversible, as given in eqn (7). Joule heat is invariably positive:[17]

$$Q_{ohm} = -i_s \cdot \nabla\phi_s - i_l \cdot \nabla\phi_l \quad (7)$$

In the eqn (7), i_s denotes the electrode current density, φ_s is the electrode potential, i_l is the electrolyte current density, and φ_l is the electrolyte potential.

Electrochemical polarization arises from the slow kinetics of electrode reactions, causing the electrode potential to deviate from its equilibrium value, as shown in eqn (8). The generation of polarization heat leads to additional energy losses, which are dissipated as heat and are irreversible. Polarization heat is invariably positive:[18]

$$Q_{pol} = a_s J_i^{Li} \eta_i \quad (8)$$

where η_i is the overpotential.

In practice, these three mechanisms are not independent but interact with each other. Reaction heat is strongly influenced by SOC and temperature, Joule heat is dominated by ohmic resistances of electrodes and electrolytes, while polarization heat becomes more significant at high current densities due to sluggish electrode kinetics. Their combined effect gives rise to complex spatiotemporal heat distributions, which necessitate simplified but effective models to describe battery thermal behavior.

In 1985, D. Bernardi[19] proposed a simplified model for calculating battery heat generation based on the external circuit characteristics of the cell. This formulation comprises two terms: the first represents the difference between the open-circuit voltage and the operating voltage, and the second accounts for the effect of the entropy change coefficient on temperature. The model assumes uniform and steady heat generation within lithium-ion batteries, expressed as eqn (9):

$$q_v = \frac{I}{V_b}\left[(U_0 - U) - T\frac{\partial U}{\partial T}\right] = \frac{1}{V_b}\left[I^2 R_b - IT\frac{\partial U}{\partial T}\right] \quad (9)$$

where I is the charge/discharge current (positive for discharge, negative for charge); V_b is the battery volume (m^3); U_0 is the open-circuit voltage (V); U is the operating voltage (V); $(\partial U/\partial T)$ is the entropy coefficient (V K^{-1}); and R_b is the internal resistance (Ω).

The internal resistance R_b is closely related to the state of charge (SOC), which varies over time. The SOC-time relationship under constant-current discharge is given by eqn (10):[20]

$$SOC = 1 - \frac{I \times t}{3600 C_N} \quad (10)$$

where t is time (s) and C_N is the rated capacity (Ah).

Thus, the Bernardi model links the three fundamental heat-generation mechanisms to macroscopic electrical parameters, enabling system-level prediction of thermal behavior. However, because it assumes uniform heat generation and constant material properties, its accuracy decreases under dynamic load conditions. This limitation has motivated the development of coupled electrochemical–thermal models that incorporate SOC, local current density, and entropy variations to more precisely capture transient heat generation and distribution in lithium-ion batteries.

3. Air cooling

Air-cooled battery thermal management systems employ airflow for heat dissipation and are primarily classified into natural-convection and forced-convection cooling.[21] For large-scale, grid-level projects, stringent requirements on system lifespan and reliability favor thermal management solutions that are technically mature, have demonstrated reliability, and entail relatively low initial investment costs. Owing to their simple structure, low cost, and ease of maintenance, air-cooled systems remain important for medium-to small-scale energy storage systems with energy densities below 150 Wh kg^{-1}. However, the low thermal conductivity of air limits the cooling capacity of air-cooled systems, particularly in high-energy-density stationary applications, potentially leading to battery-pack temperature overshoot and poor temperature uniformity. In air-cooled

 © 2026 The Author(s). Published by the Royal Society of Chemistry

Open Access Article. Published on 12 January 2026. Downloaded on 4/4/2026 5:57:19 AM. This article is licensed under a Creative Commons Attribution-NonCommercial 3.0 Unported Licence.

thermal management systems, the spatial layout of the battery array and the configuration of cooling airflow are key factors governing thermal performance.

3.1. Battery arrangement optimization

The spacing between batteries directly affects airflow velocity within the duct and the development of the thermal boundary layer, making it a critical parameter for determining both heat-dissipation efficiency and system pressure drop. Theoretical models indicate that, under constant airflow conditions, increasing battery spacing reduces flow velocity and weakens convective heat-transfer performance, whereas excessive spacing increases flow resistance. This effect can be quantified by eqn (11):

$$R_e = \frac{\rho u D_h}{\mu} \quad (11)$$

where ρ is the air density (kg m^{-3}), u is the flow velocity (m s^{-1}), D_h is the hydraulic diameter of the flow channel (m), and μ is the air dynamic viscosity (Pa s). The Reynolds number (R_e) determines the flow regime, thereby influencing the convective heat-transfer coefficient.

Gungor[22] investigated the evolution of the thermal boundary layer and heat-transfer performance under two extreme conditions—battery spacing approaching zero and infinity—*via* numerical simulations. Using the asymptotic intersection analysis method, the study showed that for R_e between 250 and 2000, the optimal battery spacing in the energy storage system ranges from 3.5 mm to 5.8 mm. This result provides a quantitative reference for the air cooling design of energy storage systems.

3.2. Cooling airflow configuration methods

Optimizing airflow configuration can enhance temperature uniformity and reduce energy consumption. Key strategies include dual-inlet/outlet structural design and the incorporation of deflector plates. A dual-inlet structure can distribute airflow more uniformly within cooling channels, thereby improving temperature uniformity.[23] Additionally, a dual-outlet structure increases the total outlet area, thereby reducing the overall power consumption of the BTMS.

Through CFD-based numerical simulations of U-shaped (Fig. 1a) and Z-shaped (Fig. 1b) air-cooled systems, Wu[24] found the U-shaped configuration to be more efficient than the Z-shaped counterpart. Following multi-objective optimization *via* the Nelder–Mead algorithm, fan power consumption was reduced from 1.51 W to 1.05 W. As shown in Fig. 1c, Luo *et al.*[25] proposed an X-type, dual-inlet, dual-outlet symmetric air-cooled battery thermal management system. Orthogonal optimization of the system's inlet and outlet parameters reduced the maximum temperature and the maximum temperature difference by 4 K and 8.09 K, respectively. Additionally, Shen *et al.*[26] designed an improved, non-vertical Z-type air-cooled system (Fig. 1d). The study found that fixing the angle between the inlet/outlet and the flow channel at 19° accelerated heat exchange between the air and the battery pack. Compared with the traditional Z-type air-cooled system, the maximum temperature decreased from 38.15 °C to 34.14 °C, and the temperature difference decreased from 2.59 °C to 1.97 °C.

Deflector plates guide airflow to ensure more uniform passage through the battery pack, thereby reducing localized overheating. Xu *et al.*[27] simulated air-cooled heat dissipation in a lithium-ion battery energy storage compartment and found poor temperature uniformity, with significant increases in the central region reaching 70.65 °C, which could markedly shorten battery component lifespan. Under the same operating conditions, adding deflector plates reduced the average temperature, maximum temperature, and temperature difference in the battery compartment by 4.57 °C, 4.3 °C, and 3.65 °C, respectively.

Although optimizing spacing and airflow configuration can reduce battery temperatures, high-energy-density applications may still require alternative cooling methods to meet heat-dissipation demands. Akbarzadeh *et al.*[28] compared the heat-dissipation performance of parallel U-shaped air-cooled systems and liquid-cooled systems with U-shaped cold plates under varying cooling media, flow rates, and temperatures at a 2 C discharge rate. The results showed that, with both fan power in the air-cooled system and pump power in the liquid-cooled system set to 0.5 W, the maximum cell temperature in the liquid-cooled system was approximately 3 °C lower than in the air-cooled system. Therefore, for a given power consumption, liquid-cooled battery thermal management systems provide lower module temperatures and superior temperature uniformity compared with air-cooled systems.

Overall, although air-cooling systems offer advantages such as structural simplicity, low cost, and ease of maintenance, their performance is fundamentally constrained by the low thermal conductivity and specific heat capacity of air, as well as the limited convective heat-transfer capability. As a result, air cooling is generally insufficient for controlling temperature rise and maintaining thermal uniformity in high-energy-density battery packs. In addition, the effectiveness of air cooling is highly sensitive to cell arrangement and airflow organization, and compact module designs are prone to local hot-spot formation, which further accelerates cell-level non-uniform aging. Therefore, air-cooling technology is more suitable for medium- and small-scale energy storage systems with relatively low energy density and modest heat-generation rates. For applications involving high energy density or high C-rate operation, the cooling capacity of air-based systems can no longer meet the stringent requirements for safety and reliability, necessitating the adoption of more efficient thermal management technologies such as liquid cooling.

4. Liquid cooling

Liquid cooling employs a liquid medium as the heat-transfer agent, removing heat from the battery through either single-phase convection or gas–liquid phase-change processes. Compared with air-cooled systems, liquid-cooling systems offer higher convective heat-transfer coefficients, superior temperature uniformity, and improved reliability, making them widely

Open Access Article. Published on 12 January 2026. Downloaded on 4/4/2026 5:57:19 AM.
This article is licensed under a Creative Commons Attribution-NonCommercial 3.0 Unported Licence.

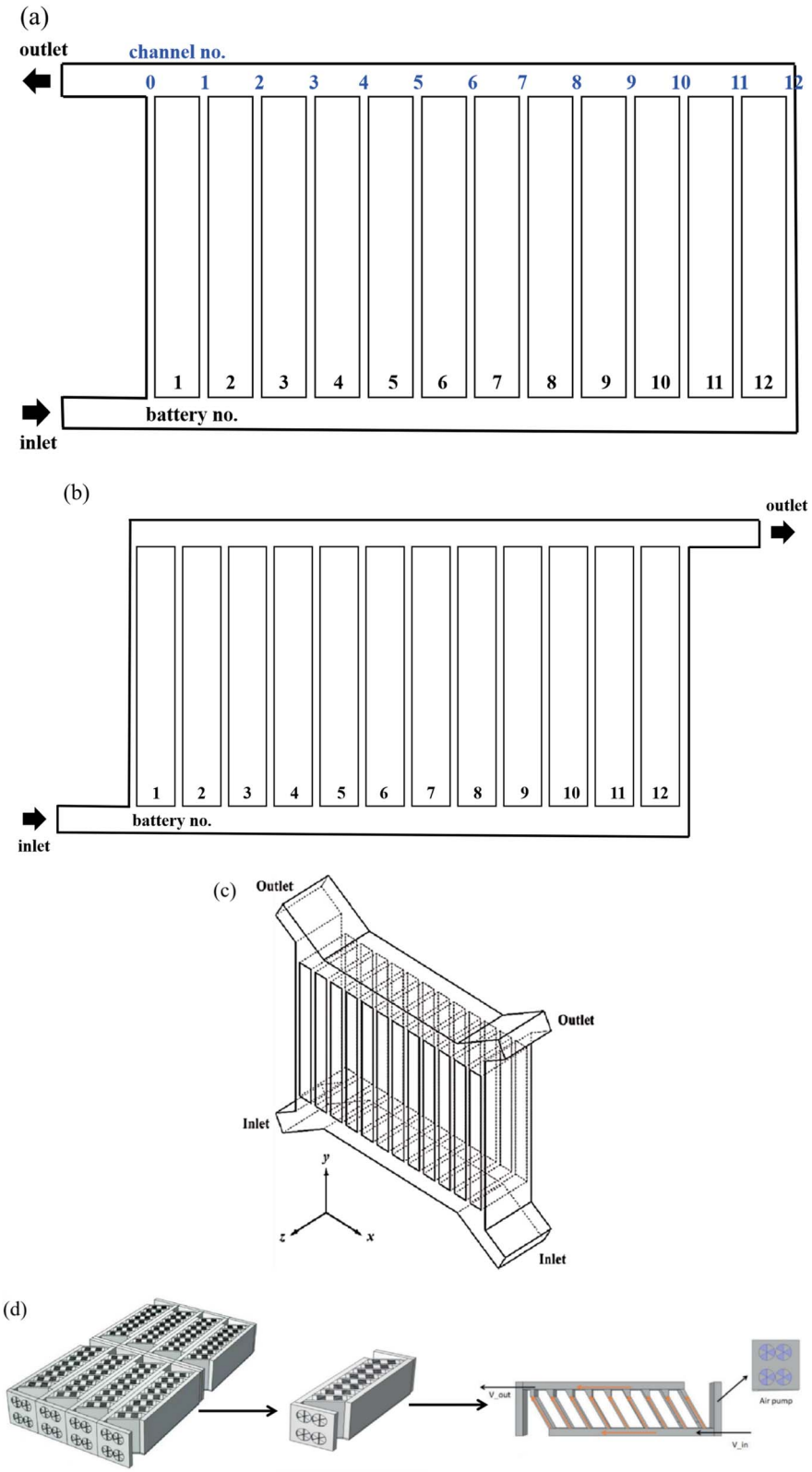

Fig. 1 (a) U-shaped air-cooling system schematic,[24] adapted from ref. 24 with permission from Elsevier, copyright 2022. (b) Z-shaped air-cooling system schematic,[24] adapted from ref. 24 with permission from Elsevier, copyright 2022. (c) X-shaped dual-inlet-dual-outlet symmetric air-cooling system schematic,[25] reproduced from ref. 25 with permission from Elsevier, copyright 2023. (d) Modified Z-shaped air-cooling system with non-vertical structure schematic.[26] adapted from ref. 26 with permission from Elsevier, copyright 2023.

© 2026 The Author(s). Published by the Royal Society of Chemistry

Open Access Article. Published on 12 January 2026. Downloaded on 4/4/2026 5:57:19 AM. This article is licensed under a Creative Commons Attribution-NonCommercial 3.0 Unported Licence.

adopted in large-scale or high-performance energy-storage applications. For example, Tesla's grid-scale energy-storage products, the Powerpack and Megapack, both employ liquid cooling. Depending on whether the cooling medium is in direct contact with the battery, liquid-cooling technologies can be classified into indirect liquid cooling (cold plate and heat pipe) and direct liquid cooling (immersion).

4.1. Cold-plate liquid cooling

Cold-plate liquid cooling is widely regarded as the most prevalent form of indirect liquid cooling and has been established as a relatively mature technology. The core component is the liquid-cooling plate, and its runner configuration plays a decisive role in governing heat-dissipation performance and temperature uniformity.[29] Common runner configurations include serpentine channels (Fig. 2a)[30] and parallel channels (Fig. 2b).[31]

The serpentine channel increases the flow path length through curved passages, thereby enhancing the heat-transfer area and capacity. However, in practice, serpentine channels often exhibit large temperature gradients along the flow direction. This phenomenon occurs because the coolant enters at a low temperature and gradually absorbs heat, leading to an elevated outlet temperature and non-uniform temperature distribution across the battery pack. Parallel channels enable simultaneous cooling through multiple flow paths, thereby enhancing cooling uniformity and decreasing flow resistance, which subsequently reduces the overall system pressure drop. Nevertheless, parallel channels may still develop considerable temperature gradients as the coolant warms downstream, which diminishes cooling effectiveness in the outlet region. To address these issues, researchers have optimized heat-exchange structures and fluid distribution strategies.

4.1.1. Enhanced heat-exchange structural design. By optimizing runner and cold-plate structural parameters—such as the number of runners, inlet coolant temperature, flow rate, and flow direction—the maximum system temperature can be reduced, temperature uniformity improved, and power consumption lowered. The convective heat-transfer coefficient can be expressed as eqn (12):

$$h = \frac{N_u \times k}{D_h} \tag{12}$$

where N_u is the Nusselt number, k is the coolant thermal conductivity (W m^{-1} K^{-1}), and D_h is the channel hydraulic diameter (m). Increasing the number of runners or incorporating disturbance features (*e.g.*, grooves, fins) enhances the Nusselt number, thereby improving convective heat-transfer performance.

The system pressure drop can be calculated as eqn (13):

$$\Delta P = f \times \frac{L}{D_h} \times \frac{\rho u^2}{2} \tag{13}$$

where f is the friction factor, L is runner length (m), ρ is coolant density (kg m^{-3}), and u is flow velocity (m s^{-1}). Optimizing runner width and depth can reduces the pressure drop (ΔP) and subsequently decreases system energy consumption.

Recent studies have demonstrated diverse approaches. Gao *et al.*[32] applied an RBF neural-network model combined with a multi-objective genetic algorithm to optimize cold-plate thickness, runner width, and the number of parallel runners, reducing maximum temperature and flow resistance by 1.9% and 13.8%, respectively. Runner width was found to have the greatest impact on cooling performance, while the number of parallel runners had the least. For ram-type parallel channels, Yu *et al.*[33] demonstrated that, within certain limits, increasing coolant flow rate, reducing runner depth, introducing spoiler features, and designing runner widths to decrease from edges to center can enhance both heat dissipation and temperature uniformity. Deng *et al.*[34] developed a U-tube serpentine-channel liquid-cooling plate and found that when the number of runners exceeded five, the incremental cooling benefit diminished. Arranging runners along the battery length yielded better cooling than widthwise layouts, while inlet temperature had minimal effect on temperature uniformity. Wang *et al.*[35] studied microchannel serpentine plates and optimized parameters using a multi-objective genetic algorithm, reducing maximum temperature by 0.85%, average temperature by 0.9%, and maximum pressure drop by 13.28%.Hu *et al.*[36] proposed a variable-flow-rate grouping strategy for serpentine channels, reducing maximum cell-to-cell temperature difference from

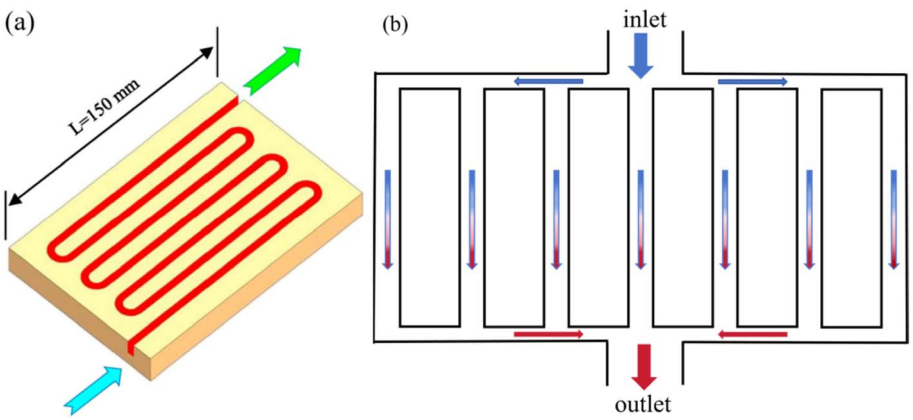

Fig. 2 (a) Serpentine channel,[30] reproduced from ref. 30 with permission from Elsevier, copyright 2018. (b) Parallel straight channel.

Open Access Article. Published on 12 January 2026. Downloaded on 4/4/2026 5:57:19 AM. This article is licensed under a Creative Commons Attribution-NonCommercial 3.0 Unported Licence.

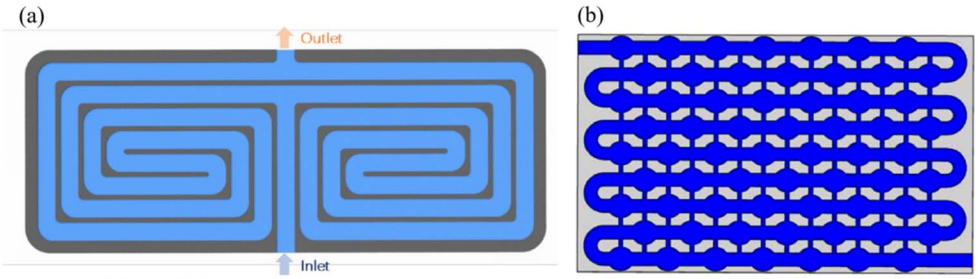

Fig. 3 (a) Parallel spiral serpentine channel schematic,[37] reproduced from ref. 37 with permission from Elsevier, copyright 2022. (b) Serpentine channel with unidirectional secondary channels and elliptical dimples schematic.[38] reproduced from ref. 38 with permission from Elsevier, copyright 2024.

2.47 K to 0.24 K and lowering maximum pack temperature from 308.78 K to 307.86 K. As shown in Fig. 3a, Guo *et al.*[37] simulated serpentine-channel performance under varying structures, flow rates, and discharge rates using STAR-CCM+, finding that parallel spiral serpentine channels offered the best overall performance. Flow rate was the dominant factor affecting maximum temperature and uniformity, while increasing channel height significantly reduced pressure drop.

Additional features such as grooves or fins can further enhance cooling. Fan *et al.*[38] incorporated unidirectional secondary channels and elliptical grooves into serpentine plates(Fig. 3b), finding that main-channel velocity and width had the strongest influence on cooling, followed by secondary-channel width and groove number. Li *et al.*[39] developed a microchannel plate with staggered circular needle fins, reducing maximum temperature rise and temperature difference by 4.045 K and 3.122 K, respectively, at a 3 C discharge rate.

Collectively, these studies confirm that runner width, flow rate, and channel geometry are dominant design factors, while auxiliary features such as grooves and fins provide supplementary enhancement of cooling performance.

4.1.2. Fluid-distribution optimization. In battery thermal management systems, battery temperature difference is closely linked to coolant temperature rise along the channel. As coolant flows downstream, its temperature increases, especially near the outlet, leading to reduced local cooling capacity. Optimizing fluid distribution can mitigate this effect.

The temperature-uniformity index is defined as eqn (14):

$$\Delta T_{\max} = T_{\max} - T_{\min} \tag{14}$$

where $T_{\max}$ and $T_{\min}$ are the maximum and minimum battery-pack temperatures (K), respectively.

Several engineered strategies have been investigated. Liu *et al.*[40] introduced cross channels into conventional serpentine layouts, finding optimal performance at seven crossovers, a 45° angle, and 2 mm width. As illustrated in Fig. 4a, Rao *et al.*[41] designed a wedge-shaped branching channel, reducing temperature difference by 35.78% at a flow rate of 1×10^{-4} m s^{-1}. Li *et al.*[42] added spoiler fins and inflow channels to serpentine parallel regions, improving coolant distribution and reducing large temperature gradients. Tang *et al.*[43] incorporated splitters (Fig. 4b)to maintain maximum cell-to-cell temperature differences below 3 °C at a 3 C discharge rate. Chen *et al.*[44] developed a secondary-flow serpentine plate(Fig. 4c), reducing inlet–outlet pressure drop by 90.69%, although maximum temperature slightly increased.

Multi-inlet/outlet systems have also shown promise. Yang *et al.*[45] found that a three-inlet, three-outlet parallel system reduced maximum temperature and temperature difference by 0.7 °C and 0.67 °C compared with a single-inlet, single-outlet design. Li and Wang[46] proposed a double-inlet, double-outlet structure with partial series connection(Fig. 5a), reducing maximum temperature by 1.285 °C and temperature difference by 1.2 °C after corner rounding, width increase, and rib shortening. Chen *et al.*[47] designed a bi-directional symmetric parallel microchannel plate, reducing temperature difference and energy consumption by 77% and 82%, respectively. As illustrated in Fig. 5b, Chen *et al.*[48] compared symmetric I-, Z-, and U-type parallel plates, finding symmetric I and Z designs to outperform symmetric U. Ren *et al.*[49] demonstrated that variable-channel microplates offered superior cooling in both single- and two-phase conditions(Fig. 5c). The same group[50] showed that variable-flow cooling better matched dynamic battery heating, enhancing latent heat contribution while reducing coolant consumption and pump power.

To further enhance liquid-cooling performance, bio-inspired structures have been proposed, which improve heat dissipation, reduce flow resistance, and lower power consumption. For instance, honeycomb and spider-web geometries increase heat-transfer area, reducing maximum battery-pack temperature and improving temperature uniformity.

Zhao *et al.*[51] designed a honeycomb-structured liquid-cooling plate for square cells. Optimization of channel width, plate thickness, center-to-boundary distance, and inlet velocity maintained maximum temperature and temperature difference at 302.5 K and 4.1 K, respectively. Reverse-direction coolant flow between adjacent plates improved temperature uniformity.

Wang *et al.*[52] developed a spider-web-channel plate (Fig. 6a) and found that channel width, number, and angle ranked in descending influence on cooling performance. Yin *et al.*[31] showed that combining spider-web-like and serpentine channels (Fig. 6b) outperformed traditional parallel layouts in heat dissipation. However, reducing inlet width and coolant temperature increased temperature difference and degraded uniformity.

© 2026 The Author(s). Published by the Royal Society of Chemistry

Open Access Article. Published on 12 January 2026. Downloaded on 4/4/2026 5:57:19 AM.
This article is licensed under a Creative Commons Attribution-NonCommercial 3.0 Unported Licence.

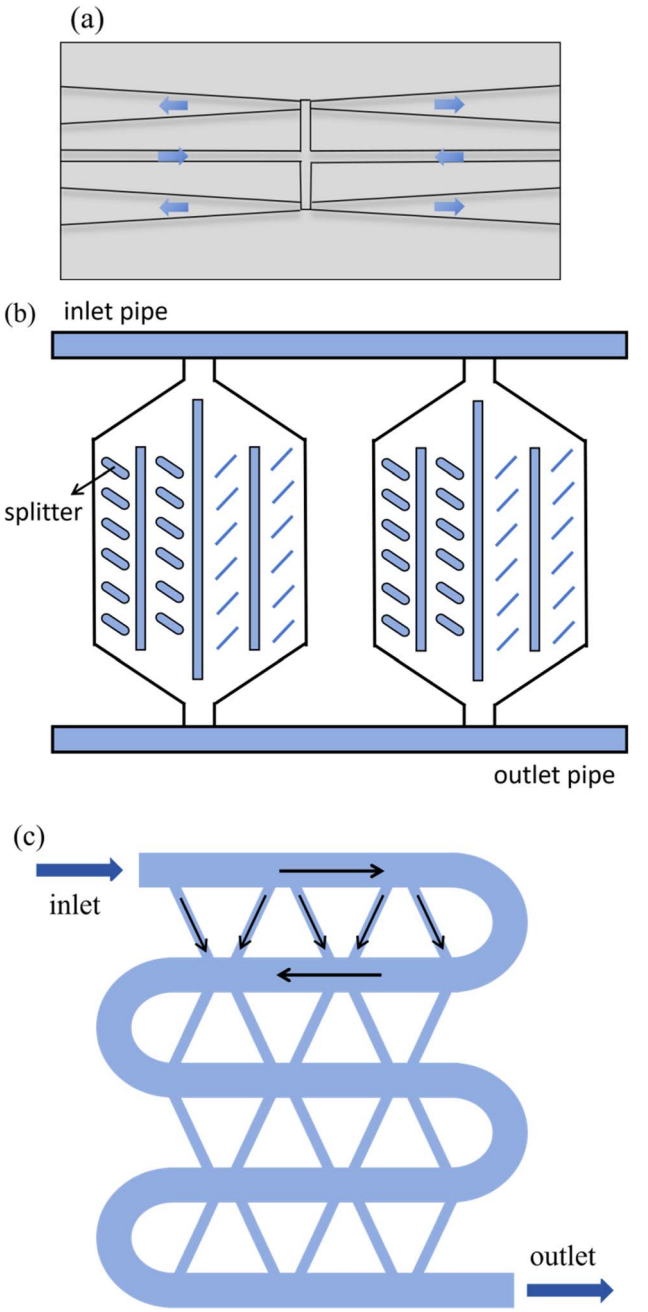

Fig. 4 (a) Modified wedge-shaped branching structure schematic,[41] adapted from ref. 41 with permission from Elsevier, copyright 2019. (b) Liquid cooling plate with flow dividers, (c) serpentine channel liquid cooling plate with secondary flow structures.

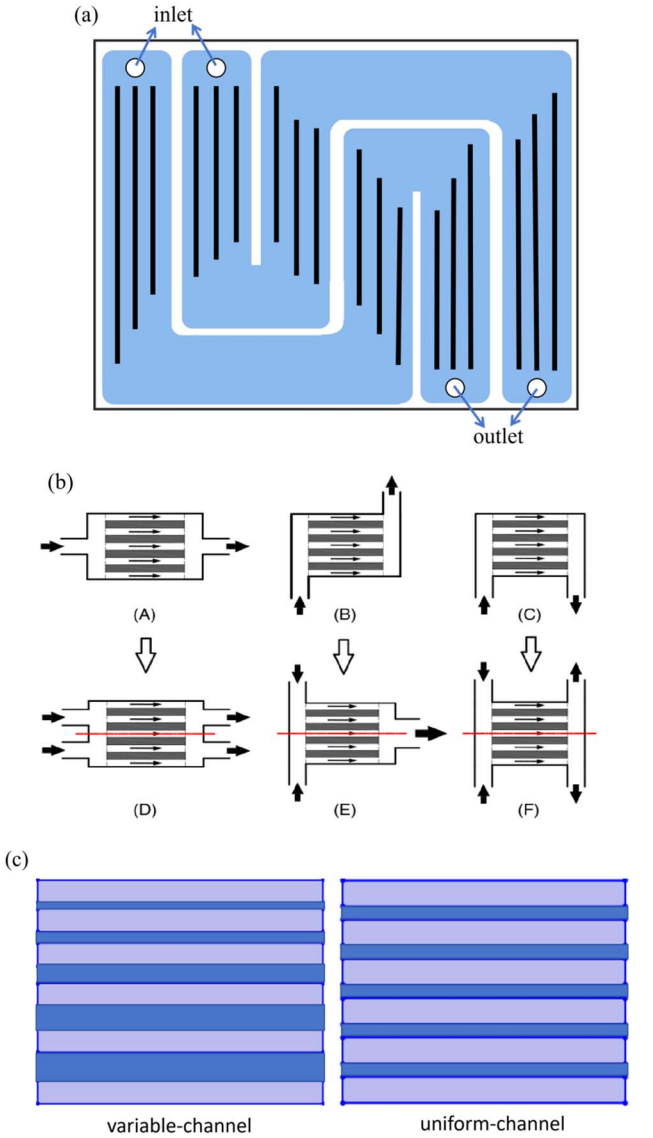

Fig. 5 (a) Optimised liquid cooling plate, (b) schematic diagrams of I-type, Z-type, and U-type parallel microchannel cooling plates before and after symmetric structure construction,[48] reproduced from ref. 48 with permission from Elsevier, copyright 2020. (c) Variable microchannel cooling plate (left) and uniform microchannel cooling plate (right).

Inspired by marine-organism streamlining, a horseshoe-crab-like fin structure reduced pressure drop and improved overall performance. As shown in Fig. 6c, Zhang *et al.*[53] found optimal results when fin size and spacing were equal in corresponding directions. Li *et al.*[54] designed a bionic blood-vessel plate that minimized fluid energy loss, with outlet spacing, plate thickness, and pipe-turning radius significantly affecting cooling. Enlarging outlet-channel area further improved performance.

Together, these findings indicate that fluid-distribution optimization—whether by engineered branching, multi-inlet/outlet systems, or bio-inspired structures—substantially enhances cooling uniformity, reduces pressure drop, and improves the overall reliability of liquid-cooled BTMS.

4.2. Submerged liquid cooling

Submerged liquid cooling is widely regarded as a highly efficient BTMS strategy, characterized by the direct contact between battery cells or associated heat exchangers and the cooling medium. This direct contact shortens the heat-transfer path, minimizes thermal resistance, and thereby yields a more uniform temperature distribution while significantly improving heat-transfer efficiency.[55,56] Owing to its high heat-transfer efficiency and excellent temperature uniformity, immersion

Open Access Article. Published on 12 January 2026. Downloaded on 4/4/2026 5:57:19 AM.
This article is licensed under a Creative Commons Attribution-NonCommercial 3.0 Unported Licence.

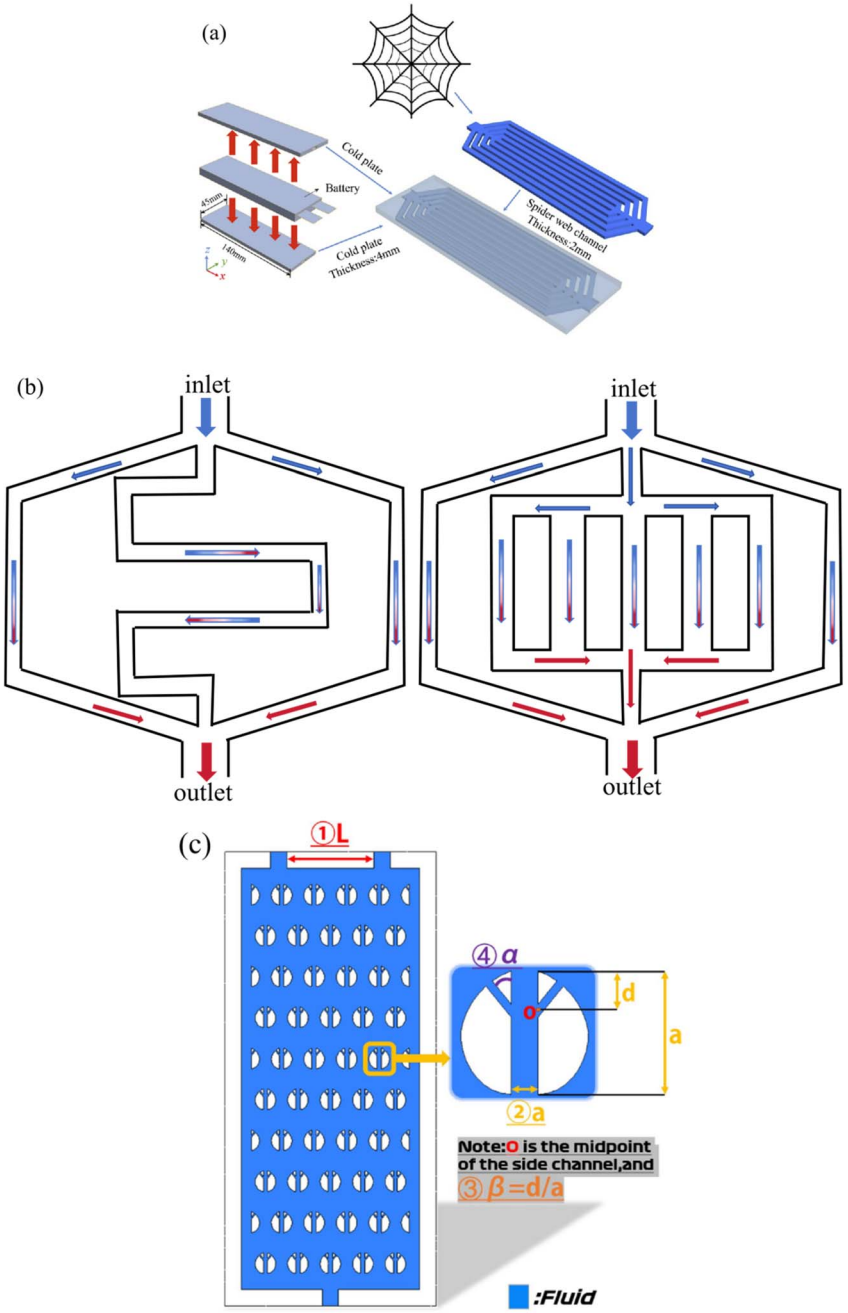

Fig. 6 (a) Cooling plate with bionic spider-web channel,[52] reproduced from ref. 52 with permission from Elsevier, copyright 2021. (b) Schematic of hybrid structure combining spider-web-inspired channels with conventional serpentine and parallel channels, (c) optimized bionic horseshoe-crab-inspired fin structure.[53] reproduced from ref. 53 with permission from Elsevier, copyright 2024.

cooling offers significant advantages in scenarios with high heat-flux density and stringent temperature-uniformity requirements.

In recent years, submerged liquid-cooling technology has attracted increasing attention as safety and efficiency requirements for large-scale energy-storage power stations have intensified, with several demonstration projects already in operation (*e.g.*, Baohu Energy Storage Station in Meizhou, Guangdong). Despite its significant theoretical and practical advantages, immersion cooling research remains at an early stage, with numerous experimental challenges still unresolved. These challenges include ensuring stable component performance under prolonged immersion, preserving coolant chemical stability after repeated use, and scaling the technology for large-scale deployment. Based on whether the cooling medium undergoes phase change within the battery's operating temperature range, immersion cooling is classified into single-phase immersion cooling and gas–liquid phase-change immersion cooling.

4.2.1. Single-phase immersion cooling. The selection of the cooling medium is a critical determinant of system performance in immersion-cooling applications. The ideal medium

© 2026 The Author(s). Published by the Royal Society of Chemistry

Open Access Article. Published on 12 January 2026. Downloaded on 4/4/2026 5:57:19 AM. This article is licensed under a Creative Commons Attribution-NonCommercial 3.0 Unported Licence.

should possess excellent electrical insulation, low viscosity, high thermal conductivity, low density, and environmental compatibility to ensure safety and sustainability.[57] In a single-phase immersion-cooling system, the cooling medium remains liquid throughout the battery's operating temperature range, without undergoing any phase change. Common single-phase cooling media include hydrocarbons (*e.g.*, mineral and vegetable oils), silicone-based oils, deionized or distilled water, and glycol-based solutions.

Direct liquid cooling using dielectric fluids offers higher cooling rates, improved safety, and reduced system power consumption and footprint. Jithin *et al.*[58] compared three dielectric fluids with air cooling and found that all maintained excellent temperature homogeneity, with deionized water outperforming mineral oil and the engineered fluid AmpCool AC-100. Nugroho *et al.*[59] demonstrated that S3 X cooling reduced surface temperature by 15.03% and maximum temperature difference by 2.5 °C at a 5 C discharge rate compared with natural cooling. Hemavathi *et al.*[60] reported that single-phase synthetic ester oil provided better cooling than mineral oil during rapid discharge, though higher flow rates (6 L min^{-1}) were required at an ambient temperature of 40 °C. Wang Zixiao *et al.*[61] found ethylene glycol to have superior cooling performance compared with silicone oil, white oil, and transformer oil; at 1 C discharge, maximum temperature and temperature difference were limited to 30.3 °C and 4.3 °C, respectively, with a system pressure drop of only 6.4 Pa.

Beyond coolant selection, optimization of cell arrangement and flow parameters within immersion modules can further reduce temperature differences and minimize pressure drop. Wang Zixiao *et al.*[61] showed that narrowing the module flow channel in the flow direction and increasing staggered-row spacing improved both cooling and hydraulic performance. Liu *et al.*[62] demonstrated that increasing cell spacing and coolant flow rate reduced temperature differences between modules under oil-immersion cooling. Liu *et al.*[63] proposed a checkerboard-topology diversion structure that enhanced coolant flow uniformity and mitigated localized hot spots. Numerical simulations indicated similar inlet–outlet pressure drops for same-side and opposite-side arrangements, but better cooling in the same-side configuration.

Uneven coolant distribution represents a persistent challenge in immersion systems. Adding baffles can help achieve uniform flow, while integrating fins can further enhance heat-transfer performance. Choi *et al.*[64] proposed a hybrid design combining channel spacers with graphite fins (Fig. 7a). Spacers ensured uniform dielectric fluid distribution, whereas high-conductivity graphite fins transferred heat from under-cooled areas, boosting overall thermal performance. Zhu *et al.*[65] compared four baffle-equipped cooling channels (Fig. 7b), identifying an optimal design that reduced maximum temperature and temperature difference by 17.9% and 20.8%, respectively, after orthogonal optimization. Huang *et al.*[66] combined finned heat pipes with static single-phase immersion cooling (Fig. 7c), achieving temperature reductions of 6.4 °C and 5.3 °C at 3 C discharge compared with natural cooling.

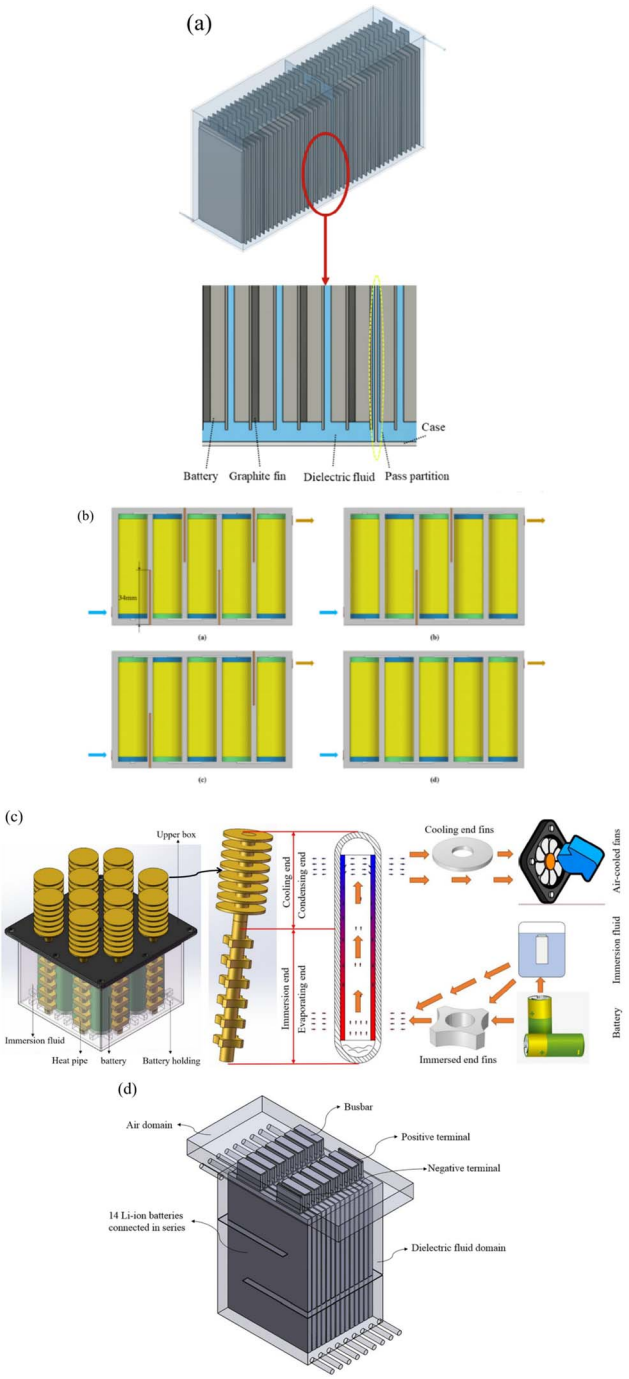

Fig. 7 (a) Hybrid immersion cooling structure featuring channel baffles and graphite fins,[64] reproduced from ref. 64 with permission from Elsevier, copyright 2023. (b) Cooling channel structure with installed baffles,[65] reproduced from ref. 65 with permission from Elsevier, copyright 2024. (c) Heat exchange schematic of finned heat pipes,[66] adapted from ref. 66 with permission from Elsevier, copyright 2024. (d) Isotropic view of dielectric fluid immersion cooling with tab cooling.[67] reproduced from ref. 67 with permission from Elsevier, copyright 2021.

Direct-contact auricular cooling has been less studied. Patil *et al.*[67] (Fig. 7d) demonstrated that immersing battery modules in flowing dielectric fluid while cooling electrode tabs reduced

Open Access Article. Published on 12 January 2026. Downloaded on 4/4/2026 5:57:19 AM. This article is licensed under a Creative Commons Attribution-NonCommercial 3.0 Unported Licence.

maximum positive-tab temperature by 46.8% (27.3 °C) compared with natural convection, highlighting the potential of targeted thermal management for critical components.

In summary, single-phase immersion cooling benefits significantly from the selection of low-viscosity, high-conductivity dielectric fluids and the optimization of flow distribution, cell arrangement, and auxiliary structures. These strategies enhance uniformity, reduce pressure drop, and improve reliability, making single-phase immersion systems highly promising for advanced BTMS.

4.2.2. Gas–liquid phase-change immersion cooling. In two-phase immersion cooling, illustrated schematically in Fig. 8, when the temperature of the coolant exceeds its boiling point, numerous small bubbles form on the cell surface.[68] As boiling progresses, these bubbles rise to the coolant surface and vaporize. If the coolant temperature is below its boiling point, some bubbles condense before reaching the surface. The vaporized coolant is condensed back into liquid *via* a condenser coil and subsequently recirculated. In this process, the coolant leverages the latent heat of the gas–liquid phase change to enhance heat dissipation and improve overall heat-transfer efficiency. By optimizing the physical properties of the coolant, temperature uniformity can be enhanced, maximum temperature rise can be effectively controlled, and battery temperature can be maintained at a stable level under high-power operating conditions. Compared with single-phase immersion cooling, two-phase cooling typically exhibits a heat-transfer coefficient several orders of magnitude higher, enabling very high heat-flux densities and excellent temperature uniformity due to the relatively constant boiling temperature. Boiling heat-transfer performance is commonly characterized by the boiling heat-transfer coefficient:

$$h_{\text{boiling}} = \frac{q}{\Delta T} \tag{15}$$

where q denotes heat-flux density (W m^{-2}) and ΔT denotes superheat (K). A higher boiling heat-transfer coefficient indicates a greater phase-change heat-transfer capability of the coolant.

As the core of an immersion-cooling system, a coolant with higher specific heat capacity and thermal conductivity, coupled with lower dynamic viscosity, promotes better temperature uniformity and facilitates effective control of maximum temperature rise. Numerous studies have focused on optimizing coolant properties to improve thermal performance. Wang *et al.*[68] and Li[69] found *via* simulation that SF33 fluid effectively maintains battery temperature within the optimal range of 33–35 °C. Li further demonstrated that ambient pressure significantly influences bubble growth and boiling point; reducing ambient pressure lowers the coolant's boiling point, thereby sustaining a constant boiling state and enhancing boiling heat-transfer efficiency. Wang *et al.*[70] reported that blending the low-boiling-point fluid R1233zd(E) with ethanol markedly enhanced boiling heat transfer from the cell wall, improving temperature uniformity of the battery module by 57%.

Williams[71] and Giammichele *et al.*[72] investigated lithium-ion batteries immersed in Novec 7000, a low-boiling dielectric fluid, and found that even under high-power charge/discharge conditions, Novec 7000 met battery temperature requirements while achieving excellent thermal homogenization. The maximum axial temperature differences were only 0.25 °C and 1 °C under 4 C charging and 10 C discharging, respectively. Lin *et al.*[73] simulated a two-phase immersion battery thermal management system under various coolant types and flow rates, concluding that R1336mzz(Z), with a high boiling heat-transfer coefficient, is suitable for high-rate discharges. Furthermore, increasing the submerged level significantly enhanced thermal safety and reduced temperature fluctuations during rapid discharge.

Wu and Liang[74] compared SF33 immersion cooling with forced air cooling, showing that SF33 provided superior heat dissipation; during 5 C dynamic discharging, temperature fluctuations under air cooling were approximately four times greater than those under immersion cooling. Li Yufeng *et al.*[75] developed a direct-immersion battery pack cooling system using Novec 7000. Results indicated that increasing coolant flow rate and cell spacing reduced both maximum top-surface temperature and maximum temperature difference, though the rate of temperature reduction diminished with further increases. Increasing the number of injection holes slightly lowered maximum top-surface temperature but significantly increased the maximum temperature difference.

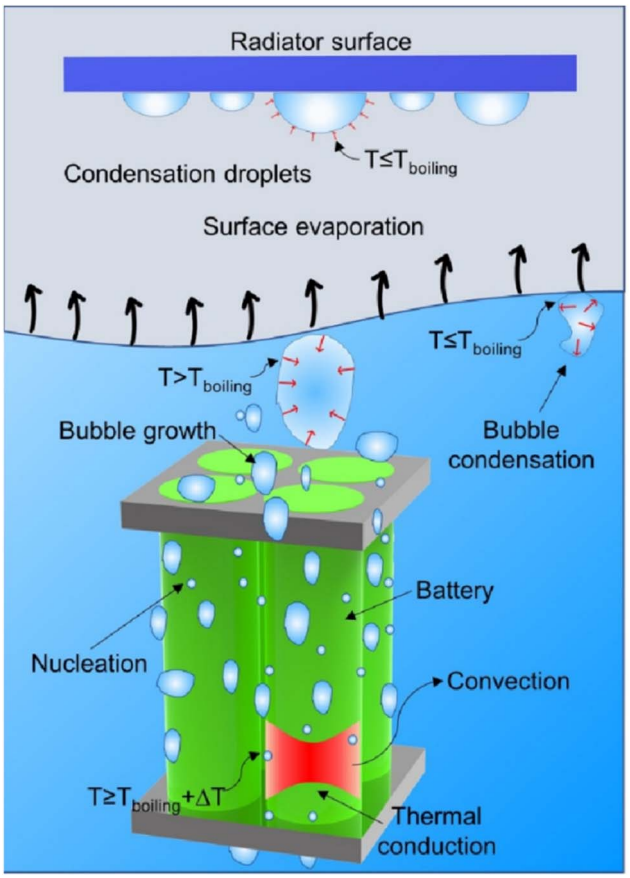

Fig. 8 Schematic diagram of boiling heat transfer[68] reproduced from ref. 68 with permission from Elsevier, copyright 2023.

© 2026 The Author(s). Published by the Royal Society of Chemistry

Open Access Article. Published on 12 January 2026. Downloaded on 4/4/2026 5:57:19 AM. This article is licensed under a Creative Commons Attribution-NonCommercial 3.0 Unported Licence.

Overall, two-phase immersion cooling utilizes latent heat transfer to achieve exceptionally high heat-transfer coefficients, maintain stable operating temperatures, and ensure excellent temperature uniformity. When properly optimized, it offers substantial improvements in safety and performance over single-phase and air cooling.

4.3. Heat pipe liquid cooling

As an efficient heat-transfer element with high thermal conductivity, excellent temperature uniformity, and structural stability, a heat pipe can be manufactured in various geometries and dimensions to meet application-specific requirements and is widely utilized in the thermal management of high-power devices. Although heat-pipe technology remains at the experimental stage for BTMS, it has demonstrated significant potential for improving heat-dissipation efficiency and maintaining optimal battery operating temperature. A schematic of a flat-plate heat pipe is shown in Fig. 9.[76]

During operation, heat generated by the battery during charging and discharging is first transferred to the heat pipe's evaporation section, where the working fluid is heated and evaporates. The vapor then flows to the condensation section, where heat is released to the surroundings *via* heat sinks or other heat-dissipating devices. After condensation, the working fluid returns to the evaporation section through gravity or capillary action, completing the cycle.

4.3.1. Heat pipe basic structure optimization. A heat pipe consists of three main components: the evaporation section, the condensation section, and the wick structure. Optimization of its geometry (*e.g.*, shape, size) and wick design can significantly enhance heat-transfer performance. The effective heat-transfer coefficient of a heat pipe can be expressed as eqn (16):

$$Q_{HP} = h_{eff} \cdot A \times \Delta T \quad (16)$$

where h_{eff} is the effective heat-transfer coefficient (W m^{-2} K^{-1}), A is the heat-transfer area (m^2), and ΔT is the temperature difference between the evaporation and condensation sections (K).

The capillary pressure generated by the wick structure can be described by eqn (17):

$$P_{cap} = \frac{2\gamma \cos \theta}{r} \quad (17)$$

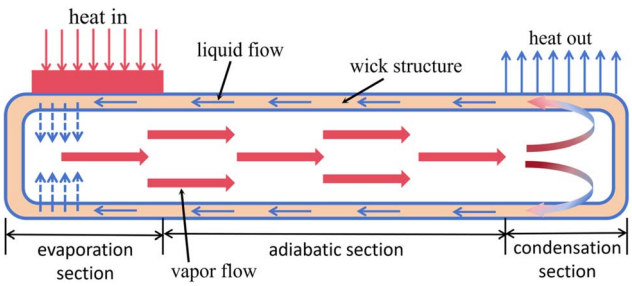

Fig. 9 Schematic diagram of flat heat pipe working principle.

where γ is the surface tension of the working fluid (N m^{-1}), θ is the contact angle (°), and r is the effective pore radius of the wick structure (m). A higher capillary pressure enhances the return flow of the working fluid.

Heat-pipe-based BTMSs are widely considered promising alternatives for maintaining the optimal operating temperature of lithium-ion batteries. Li *et al.*[77] compared liquid-cooled plates with and without heat pipes, demonstrating that optimizing channel height, length, and bending diameter reduced maximum cell temperature and temperature difference by 6.95% and 11.08%, respectively. Mbulu *et al.*[78] designed a BTMS incorporating L-type and I-type heat pipes (Fig. 10a) and showed that the system maintained maximum cell temperatures below 55 °C and temperature differences under 5 °C at 60 W input power, transferring approximately 92.18% of the battery's heat. Behi *et al.*[79] positioned heat pipes in high heat-generation regions to maximize dissipation, resulting in a 32.6% reduction in maximum temperature compared with natural air cooling, although temperature gradients increased. To address this, Behi *et al.*[80] developed a sandwiched heat-pipe cooling system (Fig. 10b) that, under forced convection, reduced maximum temperature by 33.4%.

Cooling the condenser section and selecting an appropriate coolant temperature significantly improves performance. Ye *et al.*[81] proposed an optimized BTMS for high-rate charging/discharging (Fig. 10c), showing that adding a cylindrical vortex generator before the condenser and copper fins to the heat pipe enhanced cooling and reduced non-uniformity. In another design (Fig. 10d), the evaporator was placed between two cells and the condenser inserted into a cooling channel, enabling effective heat transfer to the coolant. Liang *et al.*[82] modeled this configuration, revealing that lower coolant temperatures increased spatial gradients in local current density and Li^+ concentration, while excessively high temperatures accelerated battery aging—highlighting the need to select an optimal coolant temperature.

Wick structure properties also play a critical role in determining heat-pipe performance. Optimizing its shape, thickness, and porosity can improve working-fluid flow and heat absorption. Wang *et al.*[83] showed that both dimensionless thickness and porosity have critical values; for porosity >0.7, increasing particle size reduced maximum temperature but increased temperature difference.

Collectively, these findings confirm that heat-pipe-based BTMSs provide efficient heat transfer and temperature control, with performance strongly influenced by pipe placement, condenser cooling, coolant temperature, and wick optimization. Proper structural and operational design can substantially reduce maximum temperature and improve uniformity, making heat pipes a promising supplement to conventional liquid cooling.

4.3.2. Liquid cooling assisted heat pipe cooling. Integrating liquid cooling with heat pipes substantially enhances the overall performance of BTMS. Liquid cooling not only directly cools the battery surface but also serves as a heat sink for heat pipes, while heat pipes reduce liquid-cooling system

Open Access Article. Published on 12 January 2026. Downloaded on 4/4/2026 5:57:19 AM.
This article is licensed under a Creative Commons Attribution-NonCommercial 3.0 Unported Licence.

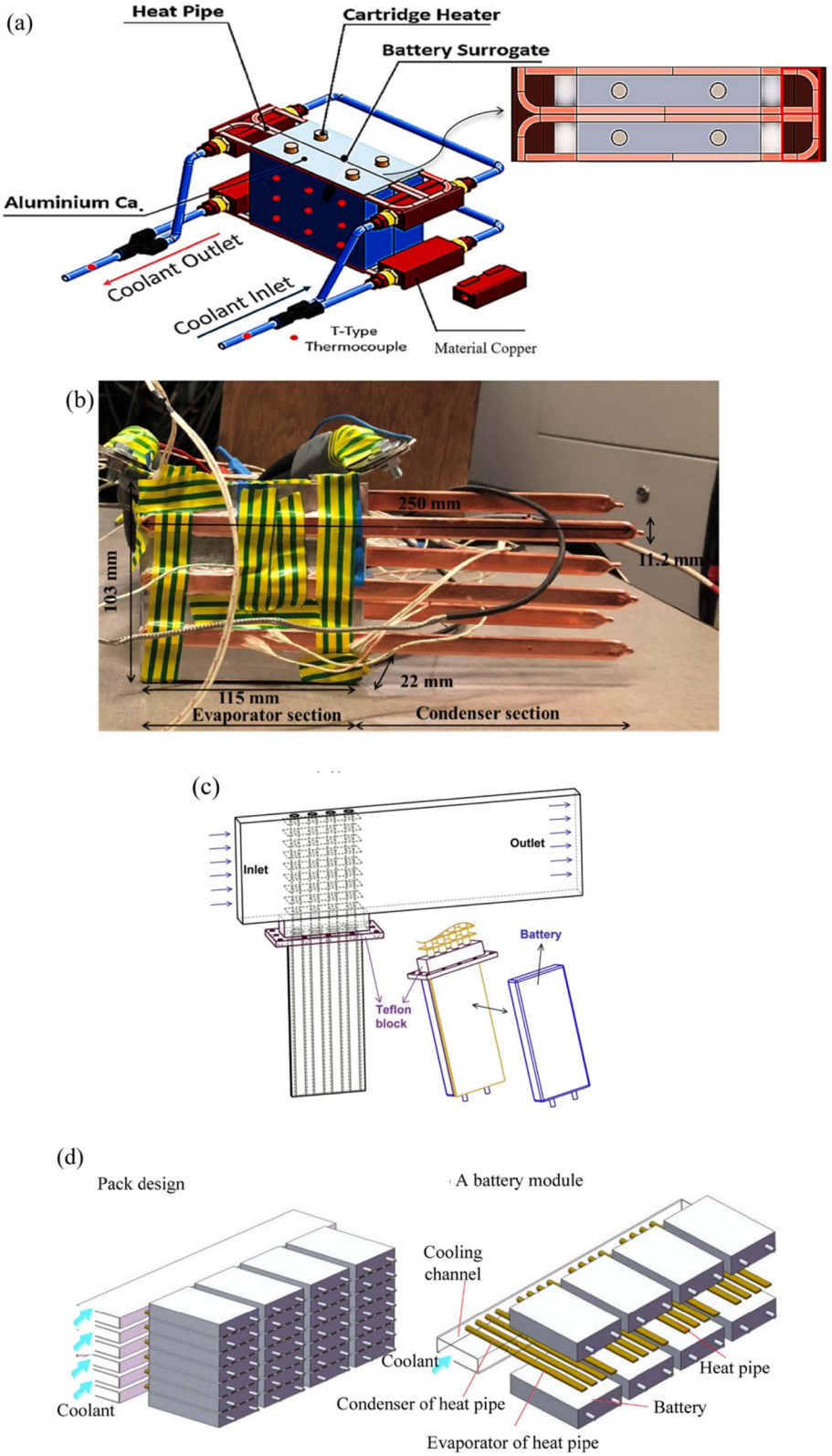

Fig. 10 (a) BTMS composed of L-type and I-type heat pipes,[78] reproduced from ref. 78 with permission from Elsevier, copyright 2021. (b) Physical diagram of sandwich heat pipe cooling system,[80] eproduced from ref. 80 with permission from Elsevier, copyright 2021. (c) Schematic of heat pipe with installed cylindrical vortex generators and copper fins,[81] reproduced from ref. 81 with permission from Elsevier, copyright 2015. (d) Heat pipe cooled battery pack design/battery module.[82] reproduced from ref. 82 with permission from Elsevier, copyright 2019.

© 2026 The Author(s). Published by the Royal Society of Chemistry

Open Access Article. Published on 12 January 2026. Downloaded on 4/4/2026 5:57:19 AM.
This article is licensed under a Creative Commons Attribution-NonCommercial 3.0 Unported Licence.

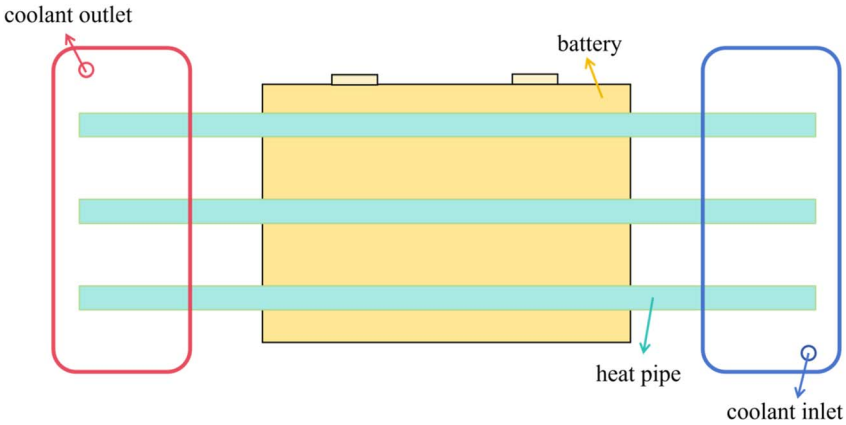

Fig. 11 Schematic diagram of hybrid liquid-cooled heat pipe system.

energy consumption and weight. This synergy increases design flexibility, boosts cooling efficiency, and prolongs battery life.

Jang *et al.*[84] proposed a hybrid system combining liquid cooling with heat pipes (Fig. 11), analyzing the effects of discharge rate, coolant mass-flow rate, coolant temperature, and ambient temperature. Optimization reduced maximum module temperature by 9.4 °C. Ma Lei *et al.*[85] found that systems with heat pipes and liquid-cooling-assisted heat pipes reduced maximum temperatures by 8.21% and 30.09%, respectively, compared with natural convection, with performance improving as coolant flow increased and temperature decreased.

Guo *et al.*[76] developed an ultra-thin flat-plate heat pipe/liquid cooling hybrid BTMS. Using one- and three-dimensional thermal models combined with orthogonal test optimization, they determined that coolant flow rate was the key parameter affecting temperature control, while heat pipe length significantly improved internal temperature uniformity.

In conclusion, hybrid BTMSs that integrate liquid cooling with heat pipes combine the high efficiency of liquid cooling and the lightweight, passive heat transport of heat pipes, thereby achieving reduced maximum temperatures, improved temperature uniformity, and decreased energy consumption. Key factors such as coolant flow rate and heat pipe length strongly govern overall system performance.

Despite the high thermal conductivity and effective temperature control offered by liquid cooling in large-scale energy storage stations, electric vehicle power batteries, and other high-heat-flux applications, the cold-plate liquid cooling systems commonly adopted in engineering practice predominantly rely on single-phase forced convection. As a result, their heat dissipation capability is inherently limited by the specific heat capacity of the working fluid, making it difficult to efficiently handle transient thermal spikes within short time scales. In addition, the structural complexity, higher maintenance requirements, and potential leakage risks restrict their ability to meet the increasing demand for enhanced safety margins in certain scenarios. Consequently, to further suppress rapid temperature rise and improve temperature uniformity, phase change material (PCM) cooling technology has attracted growing attention. Owing to its latent heat absorption during phase transition, PCM provides natural advantages in mitigating transient thermal peaks and establishes the foundation for the subsequent development of hybrid cooling strategies.

5. PCM cooling

PCM cooling technology leverages the ability of phase-change materials (PCMs) to absorb and release substantial latent heat during phase transition, thereby enabling efficient control of battery temperature.[86] PCMs effectively mitigate the rate of battery temperature rise during heat absorption and prevent excessive cooling during heat release, ensuring stable battery operation. Their primary advantages include passive operation with no active energy consumption and excellent temperature uniformity; however, their application is hindered by low thermal conductivity and high interfacial thermal resistance. PCM modules can substantially reduce both the maximum temperature and the temperature gradient of the battery at the end of discharge, while offering high heat-storage capacity and temperature uniformity.[87] Nevertheless, due to intrinsically low thermal conductivity and limited heat-storage capacity, standalone PCM systems are seldom employed as the primary cooling method in high-power or long-duration energy storage applications. Instead, they are more commonly applied for short-term peak thermal loads or integrated with active cooling systems. For residential energy storage systems with intermittent operation, PCMs have sufficient time to re-solidify during idle periods. Consequently, enhancing the thermal conductivity of PCMs has become a central focus of ongoing research.

5.1. Regulation of PCM thermal properties

The thermal regulation performance of a PCM depends primarily on its thermal properties, including the latent heat of phase change (ΔH), thermal conductivity (k), and the phase-transition temperature range. The latent heat storage capacity can be expressed as eqn (18):

$$Q_{\text{latent}} = m \times \Delta H \tag{18}$$

© 2026 The Author(s). Published by the Royal Society of Chemistry

Open Access Article. Published on 12 January 2026. Downloaded on 4/4/2026 5:57:19 AM. This article is licensed under a Creative Commons Attribution-NonCommercial 3.0 Unported Licence.

where m is the mass of PCM (kg) and ΔH is the latent heat of phase change (J kg^{-1}). A higher ΔH value increases the PCM's heat-storage capacity.

The effective thermal conductivity of a composite PCM, based on the mixing rule, is given by eqn (19):

$$k_{\text{eff}} = \varphi \times k_{\text{filler}} + (1 - \varphi) \times k_{\text{PCM}} \quad (19)$$

where ϕ is the volume fraction of high-thermal-conductivity filler (*e.g.*, expanded graphite), and k_{filler} and k_{PCM} are the thermal conductivities of the filler and matrix material, respectively.

The incorporation of fillers—such as metal powders, carbon-based materials (graphite, carbon nanotubes, graphene), and metal foams—can markedly enhance the effective thermal conductivity of composite PCMs. Expanded graphite is particularly advantageous due to its interconnected network structure, high thermal conductivity, low density, and cost-effectiveness. Acting as an adsorbent, it can retain PCM within its pores *via* capillary action, thereby increasing conductivity and reducing leakage. Yue *et al.*[88] fabricated a polyethylene glycol/expanded graphite PCM *via* melt blending, which, at a 2 C discharge rate, reduced the maximum battery temperature by 7.15 °C compared with forced air cooling and lowered the battery pack's temperature gradient by 10.98 °C. Zheng *et al.*[89] developed a hydrated salt PCM combining eutectic hydrated salts with expanded graphite. Experiments at 25 °C and 2 C discharge demonstrated that this PCM reduced the maximum single-cell temperature difference to 0.21 °C, while lowering the maximum temperature and temperature gradient between battery packs by 22.24% and 77.46%, respectively, relative to air cooling.

Ye *et al.*[90] designed a novel composite PCM featuring a dual phase-transition temperature range: nanoscale phase-change polymers provided latent heat between 31.7–42.1 °C, while polyethylene glycol contributed between 42.1–51.2 °C. The polymer framework strongly adsorbed expanded graphite, effectively preventing leakage. Under normal operating conditions (25 °C), the low-temperature phase range maintained module temperatures between 25.9–34.9 °C. In a high-temperature environment (40 °C), the high-temperature phase range limited the maximum module temperature and gradient to 49.2 °C and 2.2 °C, respectively, thus reducing thermal hazard risk.

As PCMs are predominantly solid and relatively rigid, they exhibit poor interfacial contact with battery surfaces, leading to high contact thermal resistance.[91] Flexible composite materials, however, provide superior assembly adaptability, mechanical flexibility, and structural conformity. Geng *et al.*[92] developed a flexible composite PCM (FCPCM) consisting of paraffin wax, styrene–ethylene/butylene–styrene block copolymer, and graphene. Experimental results indicated that FCPCM reduced the maximum temperature at the battery surface center by at least 1.89 °C, with increased thickness within a certain range further enhancing heat dissipation and reducing temperature gradients. Liu *et al.* proposed a novel, stable FCPCM with a leakage rate below 1%, in which contact thermal resistance decreased by 83.4% as the temperature increased from 37.35 °C to 53.41 °C. Furthermore, in both 1 C and 3 C cycling, the FCPCM module maintained a temperature difference within 1.35 °C.[93]

Incorporating fillers such as expanded graphite, metal foams, or carbon-based materials greatly improves PCM thermal conductivity, reduces leakage, and enhances cooling performance, while flexible composite PCMs address interfacial resistance by improving adaptability and reducing temperature gradients. Together, these advances enable safer and more reliable PCM-based BTMS.

5.2. Heat exchange structure optimization

In recent years, heat-exchange enhancement has been achieved by modifying PCM structures and incorporating heat-dissipation fins, thereby improving both thermal performance and temperature uniformity in BTMS. Dai *et al.*[94] proposed a porous PCM-filling structure with gradient porosity. Compared with a non-gradient configuration, the horizontal–vertical double-gradient design increased the effective thermal conductivity by 16.8%. Although this structure slightly reduced heat-storage density, it markedly enhanced heat-storage capacity and thermal conductivity, thereby improving temperature uniformity.

Jute fiber, a cost-effective, lightweight, and environmentally friendly material, has also been employed in combination with PCMs to reduce the maximum temperature, structural complexity, and power consumption of the system. As shown in Fig. 12a, Youssef *et al.*[95] experimentally demonstrated that PCM combined with jute fibers lowered the maximum temperature by 3.13 °C under cyclic load conditions compared with pure PCM cooling, while improving temperature uniformity.

The inherently low thermal conductivity of pure PCM can be enhanced by embedding fins within the PCM matrix, thereby significantly improving heat transfer. As illustrated in Fig. 12b, Liu *et al.*[96] proposed a PCM-based battery thermal management system incorporating leaf-vein fins. Results indicated that, compared with conventional rectangular fins, the leaf-vein fin design increased the temperature drop by 34.6%. The optimal overall performance was achieved when the fin volume fraction was 0.4. Ahmad *et al.*[97] designed a coupled system combining a metal-fin-enhanced PCM with air cooling, as shown in Fig. 12c, which presents an enlarged schematic of the PCM layer surrounding the battery and embedded metal fins. Numerical analyses revealed that PCM thickness, fin diameter, and fin number each exhibited an optimal value, beyond which heat-dissipation efficiency gradually declined. The coupled system successfully maintained the battery temperature below 40 °C while substantially reducing power consumption.

Structural modifications of PCMs, including gradient porosity structures, fiber reinforcement, and embedded heat-dissipation fins, effectively enhance thermal conductivity, improve temperature uniformity, and lower system energy consumption. These strategies overcome the intrinsic limitations of pure PCMs and enable more efficient and reliable BTMS operation.

Overall, PCM-based thermal management systems leverage the latent heat of phase transition to absorb a substantial

 © 2026 The Author(s). Published by the Royal Society of Chemistry

Open Access Article. Published on 12 January 2026. Downloaded on 4/4/2026 5:57:19 AM.
This article is licensed under a Creative Commons Attribution-NonCommercial 3.0 Unported Licence.

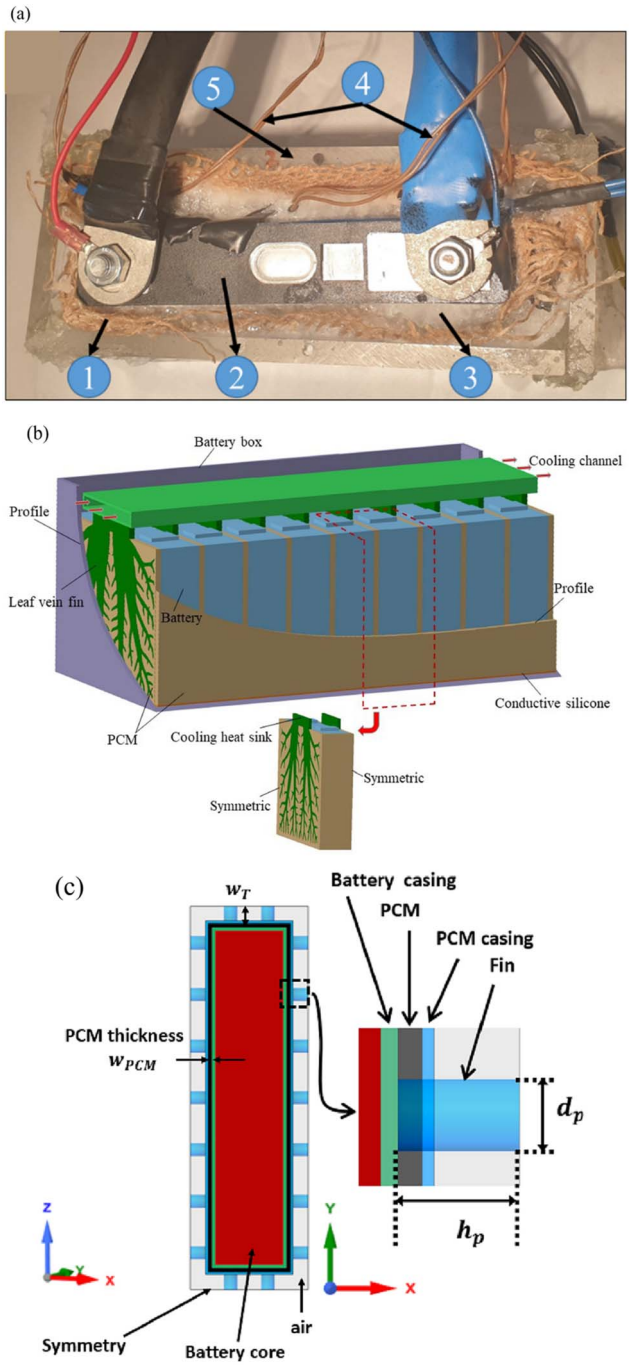

Fig. 12 (a) Cooling system integrating jute fiber with PCM,[95] reproduced from ref. 95 with permission from Elsevier, copyright 2022. (b) Battery thermal management system coupling bionic leaf-vein fins with PCM,[96] reproduced from ref. 96 with permission from Elsevier, copyright 2022. (c) Magnified view of PCM layer surrounding battery cells with embedded metal fins.[97] reproduced from ref. 97 with permission from Elsevier, copyright 2023.

amount of heat, enabling effective suppression of peak temperature rise and improvement of temperature uniformity within a short period. This makes PCM cooling particularly suitable for applications characterized by fluctuating thermal loads and strong transient cooling demands, such as high-rate charge/discharge, pulse-current operating conditions, or compact energy storage systems with limited space. In addition, PCM systems feature simple structures without pumps, offering advantages including passive safety, low noise, and high reliability. However, the inherently low thermal conductivity of most PCMs limits their ability to sustain heat removal during long-term operation. Their thermal performance is further constrained by phase-change hysteresis, volume expansion, material stability, and encapsulation challenges. Consequently, PCM cooling is more appropriate as an auxiliary method for mitigating transient thermal spikes rather than serving as the sole cooling solution for high-energy-density battery systems. Motivated by these limitations, recent research increasingly focuses on integrating PCMs with active or high-efficiency cooling techniques—such as liquid cooling, heat pipes, or microchannels—to synergistically combine transient peak-shaving capability with sustained heat dissipation, thereby enabling more efficient and safer next-generation battery thermal management systems.

6. Coupled cooling

As battery heat generation continues to intensify under high-power operation and fast-charging conditions, single-mode cooling strategies have become increasingly inadequate for simultaneously meeting the stringent requirements of peak temperature suppression, temperature uniformity, heat dissipation capacity, and energy efficiency. Coupled cooling technologies address these limitations by synergistically integrating passive and active thermal management mechanisms, enabling complementary advantages in latent-heat buffering, heat spreading, forced convection, and multi-medium heat transfer. This coordinated approach yields superior thermal regulation under complex and dynamically varying operating conditions. Based on the dominant thermal mechanisms involved, coupled cooling strategies can be broadly classified into passive-active hybrid cooling, dual-active coupled cooling, dual-passive coupled cooling, and medium-coupled cooling. Collectively, these hybrid solutions substantially expand the design space of battery thermal management and provide more robust and efficient pathways for next-generation lithium-ion batteries operating under high heat fluxes and across diverse environmental conditions. Fig. 13 illustrates the classification framework of coupled cooling technologies for lithium-ion battery thermal management.

6.1. Passive cooling + active cooling

Passive–active coupled cooling integrates passive thermal management units (such as phase change materials or heat pipes) with active heat dissipation mechanisms (such as air cooling, liquid cooling, microchannels, or thermoelectric cooling). This approach achieves a superior balance between peak suppression, sustained heat dissipation, temperature uniformity, and adaptability to operating conditions. Different passive materials possess distinct thermal properties, resulting in varied enhanced heat transfer mechanisms when integrated with active cooling. Based on material characteristics, passive-

Open Access Article. Published on 12 January 2026. Downloaded on 4/4/2026 5:57:19 AM.
This article is licensed under a Creative Commons Attribution-NonCommercial 3.0 Unported Licence.

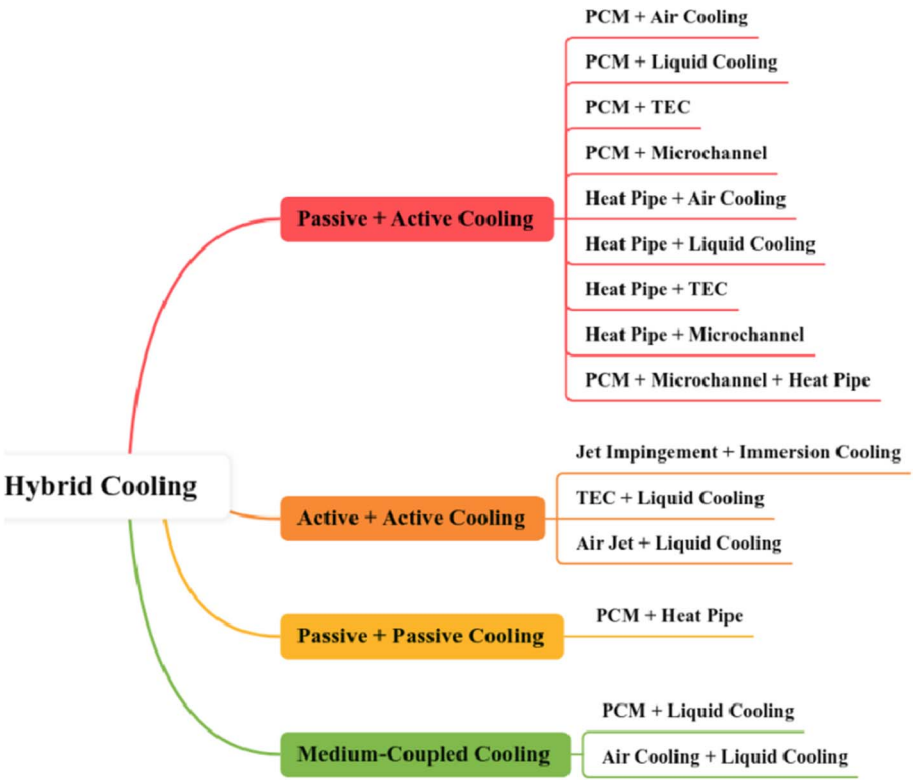

Fig. 13 The classification framework of coupled cooling technologies for lithium-ion battery thermal management.

active coupled cooling can be further categorised into three types: PCM-dominant coupled cooling, heat pipe-dominant coupled cooling, and multi-component coupled cooling systems.

6.1.1. PCM-dominated coupled cooling. PCMs possess high latent heat capacity, temperature buffering capabilities, and peak reduction potential, offering significant advantages in suppressing short-term temperature rises within batteries. When combined with active cooling (air, liquid, TEC, or microchannel), PCMs simultaneously achieve peak shaving and rapid heat dissipation, making them suitable for high-rate, dynamic electric vehicle loads with substantial temperature fluctuations.

The peak reduction capability of PCM, combined with the enhanced convection of air jets, enables the system to maintain significant cooling performance under lightweight conditions. Zhou *et al.*[98] integrated PCM with external air jet cooling to construct a hybrid thermal management system (Fig. 14a), reducing the battery's peak temperature by 26.7 °C and the temperature difference by 0.8 °C. Following optimised nozzle layout, ΔT decreased further by 49.7%, with T_{max} controlled at 34.6 °C; as wind speed increased from 12 m s^{-1} to 21 m s^{-1}, T_{max} dropped to 32.2 °C.

The PCM and liquid cooling form a complementary system: PCM buffers peak heat, while liquid cooling provides sustained dissipation. This synergy ensures exceptional thermal stability under dynamic operating conditions. Concurrently, the design flexibility of liquid cooling channel structures significantly enhances PCM utilisation efficiency. Zhang *et al.*[99] proposed a PCM-liquid cooling coupled battery thermal management system featuring a leak-proof thermal conduction channel structure. By optimising the flow channel design, the maximum battery temperature was reduced by 17.5% and the temperature difference decreased by 19.5% compared to liquid cooling alone. Chen *et al.*[100] proposed a coupled cooling system integrating a corrugated cold plate with composite PCM (Fig. 14b). By optimising cooling flow direction, PCM thickness, expanded graphite mass fraction, and phase transition temperature, the maximum battery pack temperature decreased by 22.2%, the temperature difference reduced by 16.8%, and the cell temperature difference decreased by 28.5%. Furthermore, under WLTP conditions simulating real-world driving thermal loads, this coupled system maintained stable temperature control, reducing peak battery temperatures by 20.89% compared to pure liquid cooling.

Thermal electric coolers (TECs) provide active cooling and heating, enabling PCM–TEC systems to achieve multifunctional thermal management in extreme climates through 'peak shaving + precise temperature control + low-temperature preheating'. Liao *et al.*[101] investigated the cooling performance of a battery thermal management system combining thermoelectric elements and PCM under extreme conditions (Fig. 14c). Results demonstrated that at a 3 C discharge rate, the battery's maximum temperature could be controlled below 318.15 K, with a maximum temperature difference maintained within 3 K. Liu *et al.*[102] stabilised the temperature difference at 2.5 K during 4 C discharge by optimising thermoelectric current, delayed activation strategies, and pulsed supercooling control. This

© 2026 The Author(s). Published by the Royal Society of Chemistry

Open Access Article. Published on 12 January 2026. Downloaded on 4/4/2026 5:57:19 AM.
This article is licensed under a Creative Commons Attribution-NonCommercial 3.0 Unported Licence.

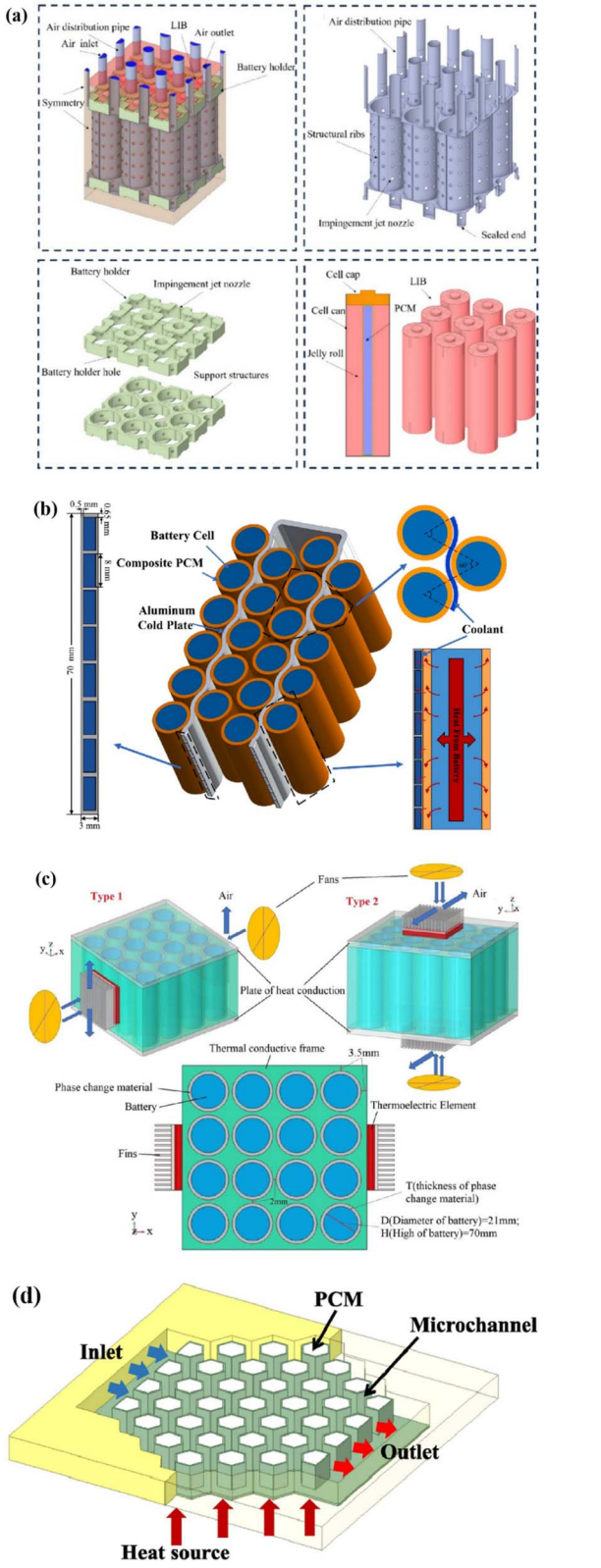

Fig. 14 (a) PCM-coupled air jet thermal management system,[98] reproduced from ref. 98 with permission from Elsevier, copyright 2024. (b) PCM-coupled liquid-cooled plate thermal management system,[100] reproduced from ref. 100 with permission from Elsevier, copyright 2025. (c) Battery thermal management system combining thermoelectric elements with PCM,[101] reproduced from ref. 101 with permission from Elsevier, copyright 2021. (d) Heat sink with PCM-encapsulated honeycomb microchannels.[106] reproduced from ref. 106 with permission from Elsevier, copyright 2023.

approach maintained efficient, low-energy temperature control below 45 °C even when PCM melting reached 80%.

Microchannel cooling possesses exceptional heat transfer capability, while PCM provides thermal buffering, enabling the system to achieve synergistic effects of low peak temperatures and high temperature uniformity under high power and high heat flux density conditions. Isfahani *et al.*[103] designed a hybrid system coupling PCM/metal foam with microchannels, comparing it against single active cooling (microchannels) and single passive cooling (PCM/metal foam). The study revealed that passive cooling achieved superior temperature uniformity but exhibited higher peak temperatures; active cooling produced lower peak temperatures but poorer uniformity. The hybrid system successfully maintained both peak temperatures and temperature gradients within acceptable limits. Ren *et al.*[104] noted that PCM alone suffices for thermal management when discharge rates remain below 2 C, but active cooling becomes essential above this threshold. Their proposed dual-microchannel quad-coldplate configuration achieved optimal cooling and temperature uniformity. Bi *et al.*[105] combined microchannel flat tubes, PCM, and artificial graphite sheets, achieving a maximum temperature of just 26.16 °C with a temperature difference of only 0.95 °C. Chen *et al.*[106] proposed a composite heat dissipation structure integrating honeycomb microchannels with encapsulated PCM (Fig. 14d). Compared to single microchannels, this system reduced overall temperatures by 2–5 K, with improved uniformity at higher flow rates. However, significant temperature rise persisted in the rear channels, indicating further structural optimisation is required. Cao *et al.*[107] incorporated a nano-PCM emulsion into composite PCM and coupled it with microchannels to create a delayed cooling strategy. This design minimized active cooling duration while maximizing passive cooling periods, thereby reducing power consumption. After optimization, the system operated for less than 25% of the total cycle time over three consecutive charge–discharge cycles.

6.1.2. Heat pipe-dominated coupled cooling. Heat pipes possess exceptionally high thermal conductivity and extremely low thermal resistance, enabling rapid dispersion of localised hotspots within batteries and reducing thermal concentration. When coupled with active cooling methods such as air cooling, liquid cooling, or microchannel cooling, they significantly enhance heat dissipation rates and temperature uniformity. This makes them suitable for high-rate, high-heat-flux-density, and locally intense thermal generation conditions.

The heat pipe rapidly disperses hotspots, while the air-cooling system offers lightweight construction and low energy consumption. This combination forms a bidirectional temperature control solution capable of both heat dissipation and low-temperature preheating. As shown in Fig. 15a, Zhang *et al.*[108] proposed a micro-heat pipe array coupled with an air-cooling system. Under 1 C and 35 °C conditions, compared to natural convection, the system's peak temperature decreased from 70.20 °C to 44.06 °C, maintaining a temperature difference within 2.76 °C. It also achieved rapid preheating from −20 °C to 20 °C within 5.4 minutes.

Open Access Article. Published on 12 January 2026. Downloaded on 4/4/2026 5:57:19 AM.
This article is licensed under a Creative Commons Attribution-NonCommercial 3.0 Unported Licence.

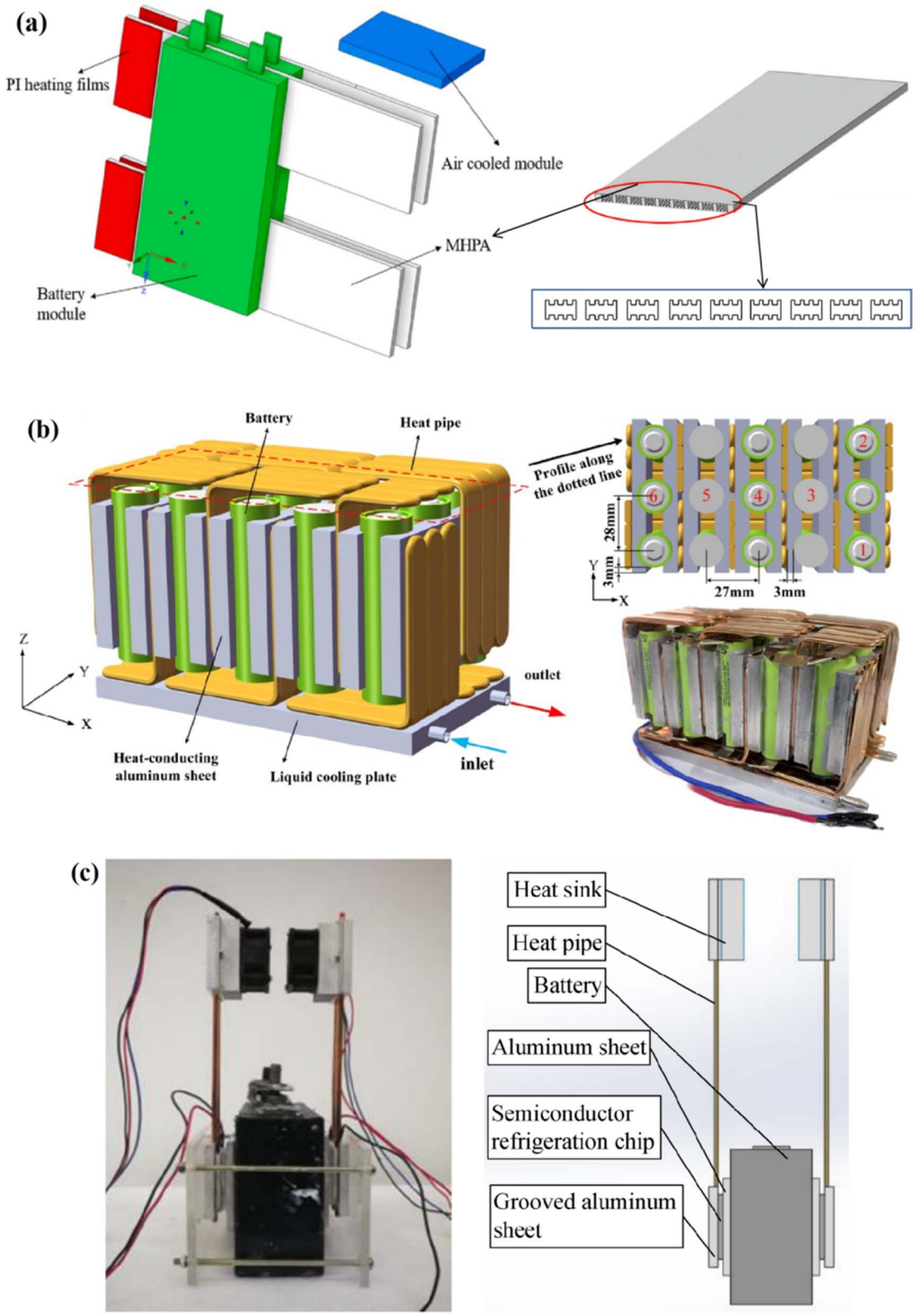

Fig. 15 (a) Micro-heat pipe array coupled with an air-cooling system,[108] adapted from ref. 108 with permission from Elsevier, copyright 2025. (b) L-shaped heat pipe-liquid cooling coupled BTMS,[109] reproduced from ref. 109 with permission from Elsevier, copyright 2024. (c) Battery thermal management system integrating heat pipes with thermoelectric coolers.[110] reproduced from ref. 110 with permission from Elsevier, copyright 2020.

© 2026 The Author(s). Published by the Royal Society of Chemistry

Open Access Article. Published on 12 January 2026. Downloaded on 4/4/2026 5:57:19 AM.
This article is licensed under a Creative Commons Attribution-NonCommercial 3.0 Unported Licence.

Heat pipes rapidly disperse hotspots, while liquid cooling swiftly removes substantial heat, enabling the system to maintain significant cooling and temperature-equalising capabilities under high-rate conditions. Zhang *et al.*[109] proposed an L-shaped heat pipe-liquid cooling coupled BTMS (Fig. 15b), reducing the battery peak temperature to 30.12 °C during 3 C discharge at 25 °C. Compared to forced air cooling and bottom liquid cooling respectively, this achieved reductions of 30.16% and 17.01% respectively, while further compressing the temperature difference to 2.02 °C, significantly enhancing temperature uniformity and heat dissipation efficiency.

Heat pipes possess exceptionally high thermal conductivity, enabling rapid hotspot diffusion, while TEC precisely regulates temperatures. This coupling renders the system particularly suitable for scenarios demanding stringent setpoint control. Zhang *et al.*[110] investigated a hybrid system integrating heat pipes and thermoelectric cooling (Fig. 15c), which effectively reduced surface temperature rise rates across multiple heat flux scales while maintaining temperatures within optimal ranges, though its uniformity slightly lagged behind natural convection.

6.1.3. Multi-coupled cooling systems. Multi-coupled cooling systems integrate multiple mechanisms such as PCM, heat pipes, and microchannels to achieve a triple synergistic effect of 'peak shaving + diffusion + forced dissipation'. This ensures stable thermal management performance across wide operating conditions, high dynamic loads, and extreme environments. As illustrated in Fig. 16, Yuan *et al.*[111] investigated a composite battery thermal management system. Intrutuegrating heat pipes, thermally conductive adhesives, PCM, and microchannel cooling plates, this system employs an optimised structural layout to substantially reduce temperature differentials across battery terminals under high-temperature conditions while rapidly heating to operating temperatures during low-temperature cycles. At 0 °C ambient temperature, this system elevated the battery temperature to 20 °C within approximately 1500 seconds, with near-stable temperature variation demonstrating its efficient heating capability.

6.2. Active + active cooling

Active–active coupled cooling provides the highest heat removal capacity under conditions of extremely high heat flux density, transient thermal shocks, and high-rate rapid charging/discharging by superimposing two enhanced heat transfer mechanisms. Such systems effectively disrupt thermal boundary layers, substantially reduce local hotspot temperature rises, and maintain stable overall temperature control. They are suitable for high-power batteries, electric vehicle rapid charging, and aerospace batteries.

Jet cooling employs high-velocity jets to effectively break thermal boundary layers, significantly enhancing local heat transfer coefficients. Immersion cooling ensures uniform heat dissipation across large areas. The combination of both offers exceptional advantages when addressing hotspots with high

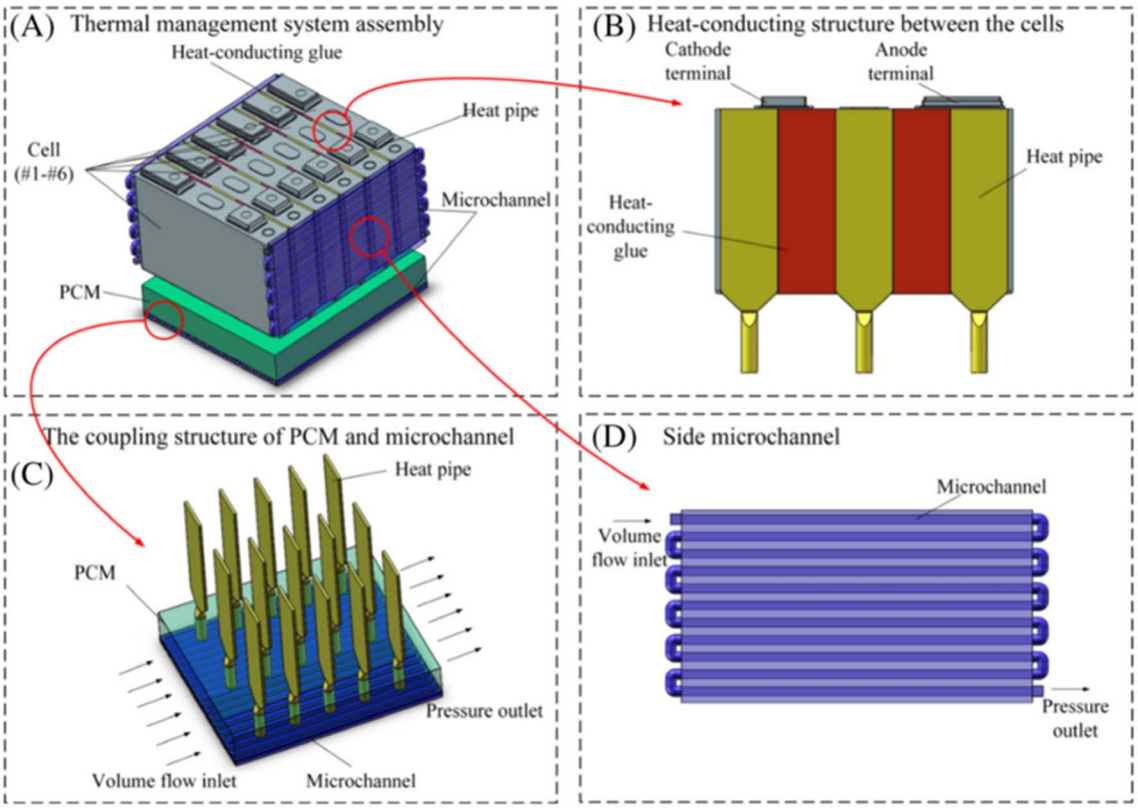

Fig. 16 Geometric model of a hybrid battery thermal management system.[111] reproduced from ref. 111 with permission from John Wiley and Sons, copyright 2020.

Open Access Article. Published on 12 January 2026. Downloaded on 4/4/2026 5:57:19 AM.
This article is licensed under a Creative Commons Attribution-NonCommercial 3.0 Unported Licence.

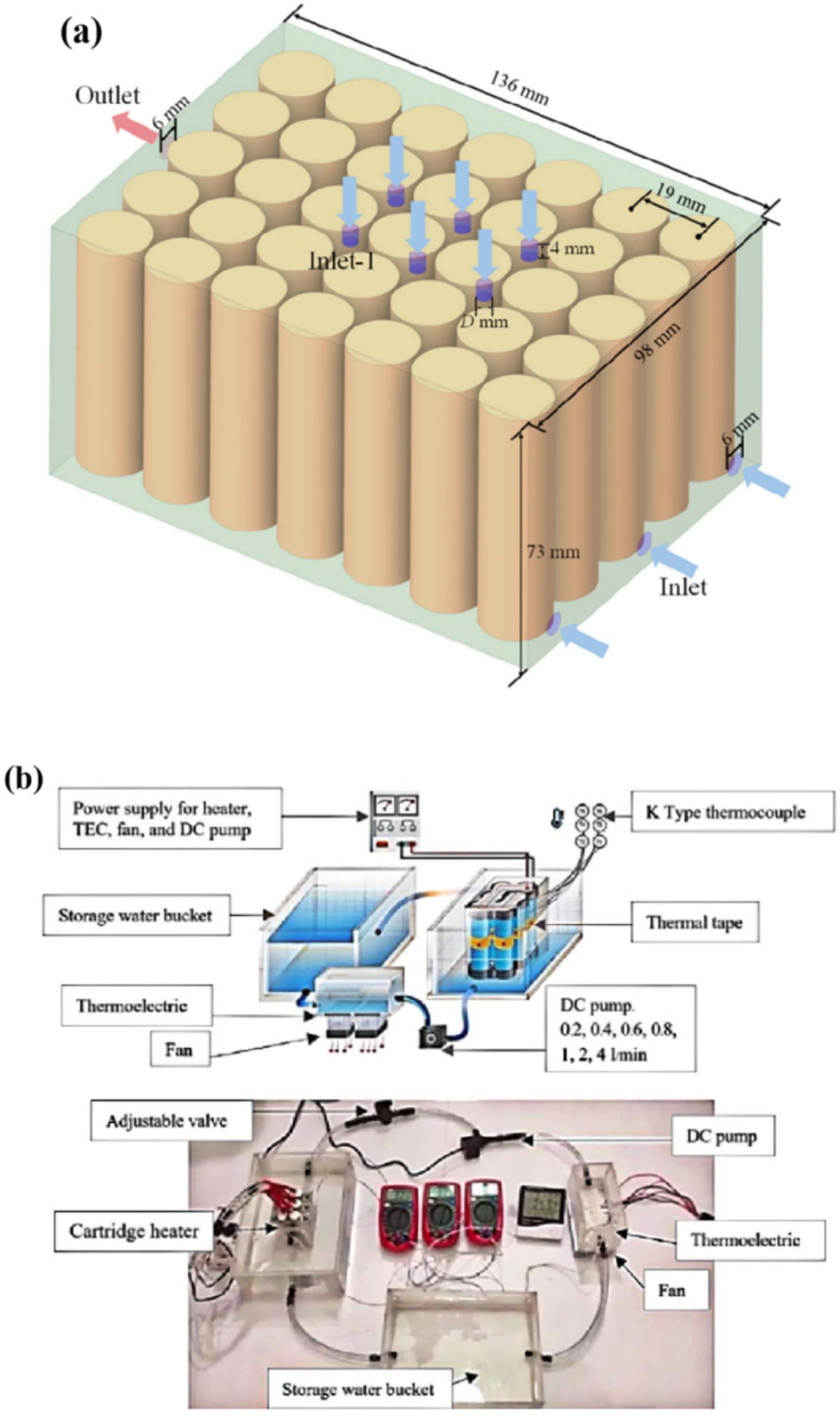

Fig. 17 (a) Jet-impact coupled immersion-cooled battery thermal management,[112] reproduced from ref. 112 with permission from Elsevier, copyright 2024. (b) TEC-liquid cooling coupled system.[114] reproduced from ref. 114 with permission from Elsevier, copyright 2024.

heat flux densities. Song *et al.*[112] proposed an innovative battery thermal management strategy coupling jet impact with immersion cooling(Fig. 17a). By adjusting flow distribution, jet tube quantity, and dimensions, they substantially reduced lithium battery peak temperatures, temperature differentials, and cooling system energy consumption. Zhang *et al.*[113]

© 2026 The Author(s). Published by the Royal Society of Chemistry

Open Access Article. Published on 12 January 2026. Downloaded on 4/4/2026 5:57:19 AM.
This article is licensed under a Creative Commons Attribution-NonCommercial 3.0 Unported Licence.

designed an immersed array jet cooling system. After optimising the nozzle spacing (42.6 mm × 34 mm), the maximum temperature of the battery heat plate was controlled at approximately 32–33 °C, with the temperature difference compressed to around 5–7 °C. Optimal heat transfer performance was achieved within a flow rate range of 1–1.5 L min^{-1}, significantly enhancing cooling efficiency and temperature uniformity.

TECs possess controllable cooling capabilities, enabling precise surface temperature regulation, while liquid cooling rapidly dissipates heat extracted by the TEC. This combination delivers exceptionally high cooling rates and stable controllability under high-power charging/discharging conditions. As depicted in Fig. 17b, Panmuang *et al.*[114] developed a TEC-liquid cooling coupled system. By regulating the synergistic effect of TEC refrigeration and water cooling across a 0–4 L min^{-1} flow range, they reduced battery surface temperatures by approximately 41–52% compared to standalone air or liquid cooling. The most pronounced cooling effect was observed at discharge rates of 1–3 C.

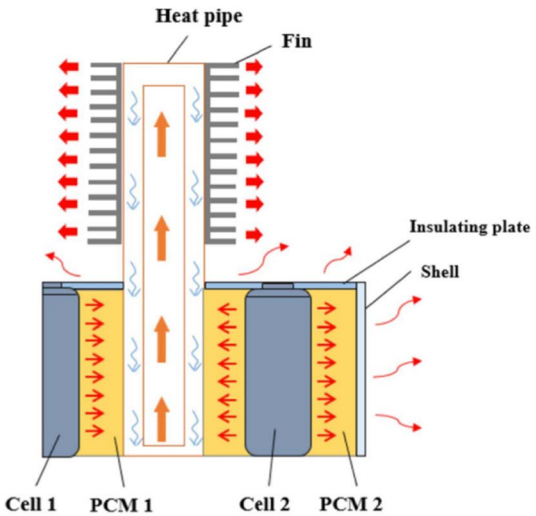

Fig. 18 Simplified heat transfer process schematic of heat pipe coupled PCM cooling.[115] reproduced from ref. 115 with permission from Elsevier, copyright 2022.

6.3. Passive cooling + passive cooling

Passive–passive coupled cooling requires no external energy input, rendering the system safer, more reliable, and lower in maintenance costs. It is suitable for energy-sensitive, structurally compact, or medium-heat-flux-density applications.

Heat pipe/PCM coupled cooling technology leverages the high thermal conductivity of heat pipes and the substantial latent heat storage capacity of PCM, offering significant energy-saving potential alongside enhanced heat dissipation performance. A simplified schematic of the heat transfer process is illustrated in Fig. 18.[115] Within this system, heat generated by the battery is first absorbed through the phase change of the PCM, thereby reducing the rate of temperature rise; subsequently, the heat pipe rapidly dissipates the accumulated heat from the PCM, accelerating heat removal and preventing PCM saturation, thereby enhancing overall cooling efficiency.

Under ambient temperatures of 25 °C and 40 °C, comparisons between air cooling, PCM cooling, and heat pipe/PCM coupled cooling (Fig. 19)[115] reveals that at 25 °C, PCM cooling alone suffices for thermal management requirements. However, at 40 °C, the PCM's low thermal conductivity impedes timely heat dissipation, rendering standalone PCM cooling inadequate to maintain temperatures within permissible limits during the first cycle. Incorporating heat pipes accelerates internal heat transport within the PCM, significantly enhancing thermal dissipation performance.

Behi *et al.*[116] compared the performance of natural convection, heat pipe cooling, and PCM-assisted heat pipe cooling under 8 C rapid discharge conditions. The PCM-heat pipe

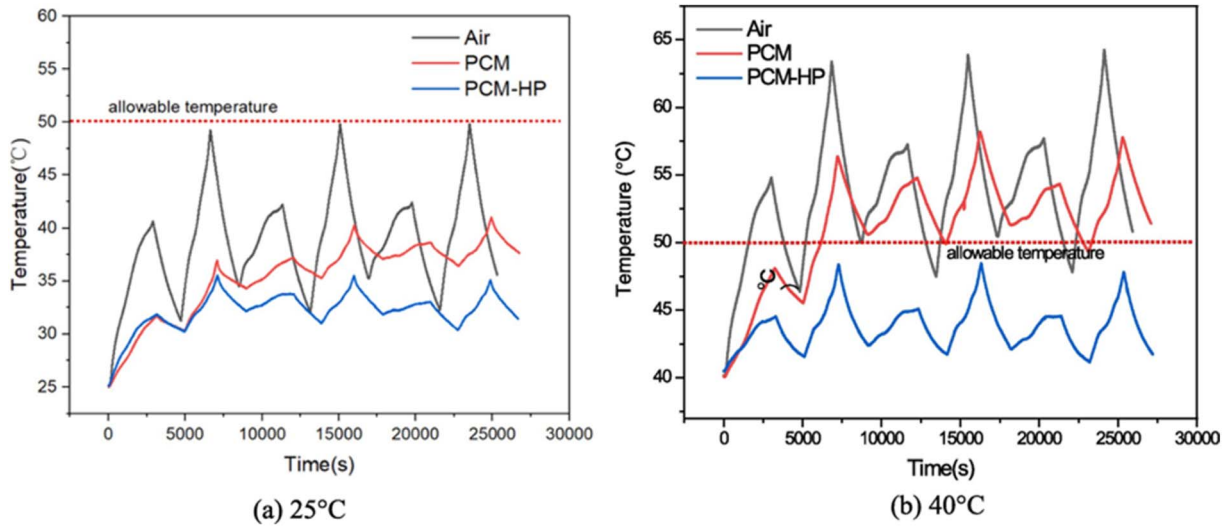

Fig. 19 Maximum temperature variations in air cooling, PCM cooling, and heat pipe-coupled phase change material cooling experiments at 25 °C and 40 °C[115] reproduced from ref. 115 with permission from Elsevier, copyright 2022.

Open Access Article. Published on 12 January 2026. Downloaded on 4/4/2026 5:57:19 AM.
This article is licensed under a Creative Commons Attribution-NonCommercial 3.0 Unported Licence.

system reduced the peak temperature to 33.2 °C, representing a 40.7% decrease compared to natural convection. Leng *et al.*[117] conducted multi-cycle testing on an optimised heat pipe/PCM system, demonstrating that PCM provided a 'peak shaving and valley filling' effect, achieving an optimised maximum energy saving rate of 81.8%. Tang *et al.*[118] investigated a paraffin/copper foam composite PCM coupled with a flat plate heat pipe system, finding superior high-temperature control performance with an optimal foam porosity of 40–50%. Putra *et al.*[119] compared multiple PCMs, concluding that RT 44HC with higher latent heat exhibited optimal performance within the 25–55 °C range, reducing maximum temperatures by 33.42 °C compared to beeswax.

6.4. Medium-coupled cooling

Medium-coupled cooling achieves a balance between heat dissipation capacity, temperature uniformity, energy consumption, and structural complexity by integrating different cooling media (air, liquid, PCM, *etc.*). Such systems feature

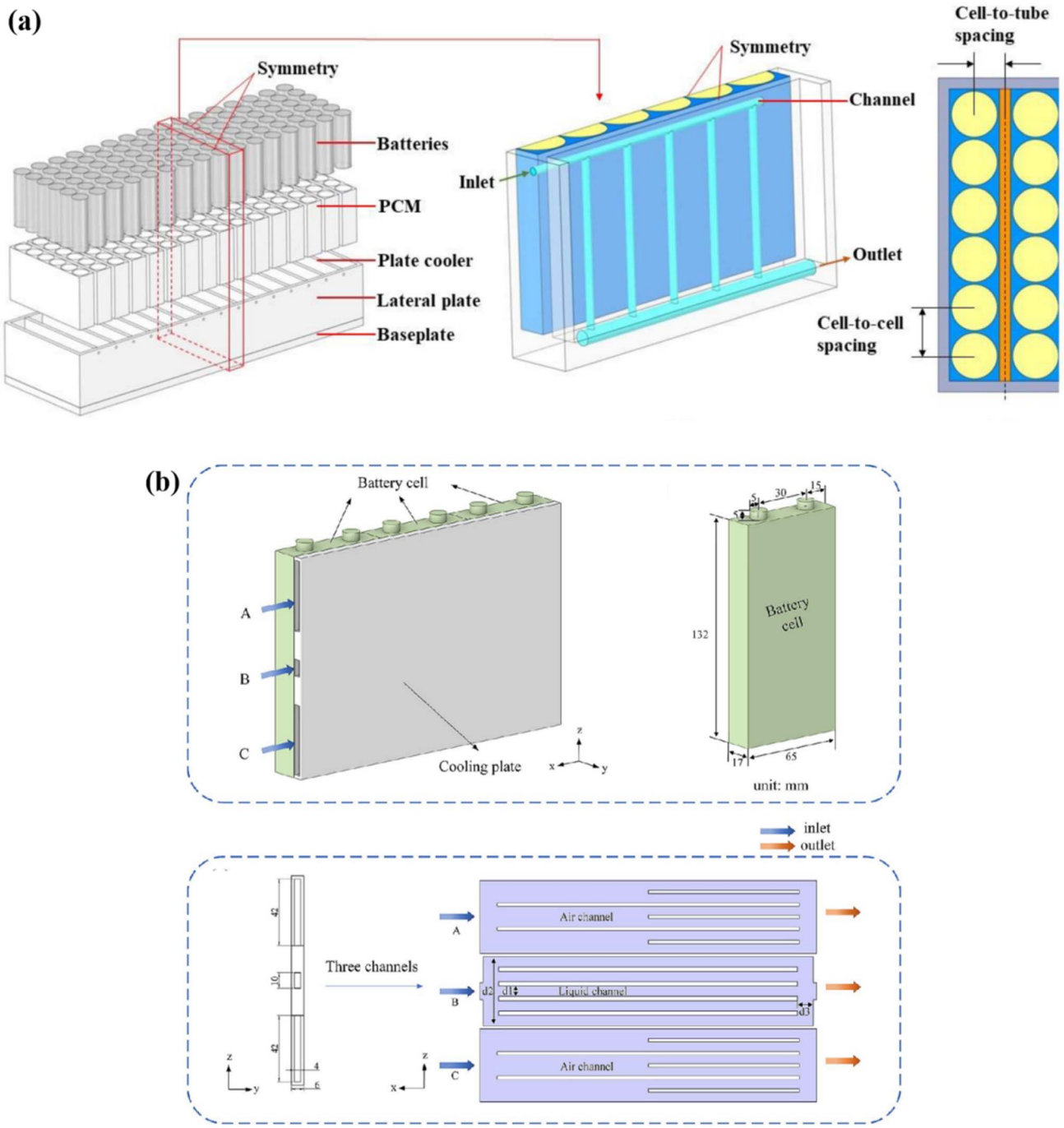

Fig. 20 (a) PCM-microchannel liquid cooling coupled system,[121] adapted from ref. 121 with permission from Elsevier, copyright 2023. (b) Air-liquid coupled cooling (ALCC) system.[122] reproduced from ref. 122 with permission from Elsevier, copyright 2025.

© 2026 The Author(s). Published by the Royal Society of Chemistry

Open Access Article. Published on 12 January 2026. Downloaded on 4/4/2026 5:57:19 AM. This article is licensed under a Creative Commons Attribution-NonCommercial 3.0 Unported Licence.

complementary thermal conductivity, heat capacity, and flow characteristics across different media, enabling efficient heat dissipation, peak-shaving capabilities, and low energy consumption. They are suitable for engineered applications requiring optimised performance-to-energy-consumption trade-offs.

Microchannels offer advantages in enhanced turbulence and localised heat transfer, while PCMs further delay battery temperature rise and suppress peaks. Their combination achieves optimal synergy between safety and thermal performance. Wang *et al.*[120] developed a PCM-corrugated microchannel liquid cooling coupled system. By enhancing heat dissipation and improving PCM utilisation through corrugated microchannels, the maximum temperature was further reduced compared to straight-channel liquid cooling, with the temperature difference narrowing to approximately 1.6 K. The incorporation of a composite PCM containing 10% graphite further lowered temperatures and delayed the burst time by approximately 440–650 s under thermal runaway conditions, significantly enhancing safety and temperature uniformity. As shown in Fig. 20a, Zhang *et al.*[121] proposed and simulated a PCM-microchannel liquid cooling coupled system. By optimising cell spacing (23 mm), cell-cold plate distance (3.5 mm), and cold plate flow channel layout. This stabilised peak temperatures within approximately 46–50 °C during three consecutive 2 C discharge/0.5 C charge cycles, controlled temperature change rates below 0.8%, and restored temperatures to below 30 °C at the end of each cycle. This effectively prevented thermal runaway and enhanced system sustainability.

Air cooling offers advantages in weight reduction and low energy consumption, while liquid cooling provides efficient heat transfer capabilities. Combining both enables significant energy savings while maintaining thermal performance. Liu *et al.*[122] proposed an air-liquid coupled cooling (ALCC) system(Fig. 20b). By introducing forced air channels on both sides of the liquid cooling plate and optimising the channel structure, the system achieves nearly identical thermal performance to pure liquid cooling during 2 C discharge with only one-third of the liquid cooling energy consumption. Furthermore, peak temperature was reduced by 1.0%, a temperature difference reduction of 8.8%, and a 22% decrease in energy consumption.

In summary, coupled cooling technology achieves multidimensional synergistic optimization between peak suppression, temperature uniformity, heat dissipation capacity, energy consumption, and structural complexity by integrating diverse passive and active thermal management mechanisms:PCM-dominant coupled systems excel in peak reduction and temperature fluctuation suppression; heat pipe-dominant coupled systems demonstrate clear advantages in hotspot diffusion and efficient thermal conduction; active–active coupled systems provide the highest level of heat exchange capability, suitable for transient high-power scenarios; while medium-coupled systems achieve the optimal balance between thermal performance and engineering feasibility.

As battery systems achieve ever-higher energy densities, demand for rapid charging grows, and requirements for all-climate adaptability increase, future coupled cooling technologies will evolve towards lightweight designs, intelligent flow and energy consumption regulation, multi-field coupling optimisation, and modular integrated structures. This progression will address the heightened demands for safety and longevity in next-generation high-performance battery systems.

7. Conclusion

An efficient thermal management system for lithium-ion batteries ensures operation within the optimal temperature range, prolongs service life, and rapidly responds to localized thermal runaway, thereby preventing propagation and mitigating further escalation. This work first analyzed the heat-generation mechanisms of lithium-ion batteries, then systematically reviewed the principles, technical characteristics, and potential research directions of individual cooling technologies, including air cooling, liquid cooling, and solid–liquid phase-change material cooling. Finally, the latest advancements in multi-coupled cooling technologies were discussed. The main conclusions are as follows:

(1) Air cooling technology, the most fundamental method, provides advantages of structural simplicity and low cost. However, its limited heat dissipation capacity makes it suitable primarily for residential or small-scale commercial energy storage systems. With the increasing energy density of batteries, air cooling is insufficient for high-power applications. Future research should prioritize optimization of battery spacing, airflow channel geometry, and inlet/outlet configurations to improve cooling efficiency.

(2) Liquid cooling technology, currently the mainstream approach, includes cold-plate liquid cooling, immersion liquid cooling, and heat-pipe-assisted liquid cooling. For cold-plate liquid cooling, optimization should target both heat-exchange structure enhancement and fluid-distribution design to minimize temperature gradients. Immersion cooling exhibits high potential due to direct contact between the coolant and batteries; however, future efforts should emphasize environmentally benign, high-performance, and cost-effective coolants, along with optimized flow-path designs. In heat-pipe-assisted liquid cooling, performance can be improved by optimizing structural and wick configurations.

(3) PCM-based cooling technology offers superior temperature uniformity and heat-storage capability, yet is limited by low thermal conductivity and high interfacial resistance. Research should focus on improving material thermal conductivity, enhancing leakage resistance, and optimizing structural integration.

(4) Coupled cooling technology integrates the strengths of multiple approaches to provide flexible and efficient thermal management, satisfying both temperature control and uniformity requirements. Future development is anticipated to progress toward intelligent, multi-physics optimization, offering substantial potential for managing high-energy-density lithium-ion batteries.

Future battery thermal management should prioritize intelligent low-temperature control, sustainable cooling media, and

Open Access Article. Published on 12 January 2026. Downloaded on 4/4/2026 5:57:19 AM. This article is licensed under a Creative Commons Attribution-NonCommercial 3.0 Unported Licence.

the establishment of standardized evaluation frameworks. Intelligent thermal regulation requires integrating advanced sensing, data-driven prediction, active flow and energy control, and real-time fault diagnosis to enable adaptive heat management under dynamic operating conditions. The selection of future cooling media should comply with environmental criteria such as zero ozone depletion potential (ODP = 0) and low global warming potential (GWP < 150), while also considering toxicity, flammability, thermal properties, and material compatibility. As cooling architectures become increasingly diverse, developing unified performance metrics, safety standards, and durability testing protocols will be essential for practical deployment. These directions collectively support the development of safer, more efficient, and more sustainable thermal management systems for next-generation high-energy-density lithium-ion batteries.

Author contributions

Zhang Qianqian: writing – original draft. Zhang Wei: writing – review & editing, supervision, conceptualization. Wang Siyang: investigation. Yang Xufei: investigation. Liu Guanglin: validation. Sun Dongliang: methodology. Yu Bo: supervision, conceptualization.

Conflicts of interest

The authors declare no conflicts of interest.

Data availability

No primary research results, software or code have been included and no new data were generated or analysed as part of this review.

Acknowledgements

The authors acknowledge the financial support from the National Natural Science Foundation of China (52076015, U2141218, 52106073).

References

1 W. Sharmoukh, Redox flow batteries as energy storage systems: materials, viability, and industrial applications, *RSC Adv.*, 2025, **15**(13), 10106–10143.
2 Md Mahmud, K. S. Rahman and Md. Rokonuzzaman, Lithium-ion battery thermal management for electric vehicles using phase change material: A review, *Results Eng.*, 2023, **20**, 101424.
3 N. Muhammad Waqas, I. Naseem and A. Majidi, Thermal management of Li-ion battery by using active and passive cooling method, *J. Energy Storage*, 2023, **61**, 106800.
4 X. Yang, H. Weibiao and G. Deng, Research Progress on Thermal Management Technology for Pure Electric Vehicle Batteries, *J. Dongguan Univ. Technol.*, 2024, **31**(01), 86–93.
5 D. Shi, Y. Cui and X. Shen, A review of the combined effects of environmental and operational factors on lithium-ion battery performance: temperature, vibration, and charging/discharging cycles, *RSC Adv.*, 2025, **15**(17), 13272–13283.
6 R. Khalid, A. Shah and M. Javed, Progress and obstacles in electrode materials for lithium-ion batteries: a journey towards enhanced energy storage efficiency, *RSC Adv.*, 2025, **15**(20), 15951–15998.
7 Z. Tang, W. Shoucheng and L. Zhiqing, Numerical analysis of temperature uniformity of a liquid cooling battery module composed of heat-conducting blocks with gradient contact surface angles, *Appl. Therm. Eng.*, 2020, **178**, 115509.
8 X. Qianqian, Y. Tianqi and Z. Hengyun, Experimental and numerical study of lithium-ion battery thermal management system using composite phase change material and liquid cooling, *J. Energy Storage*, 2023, **71**, 108003.
9 M. Talha, R. Palange and S. A. Khan, Mitigating thermal runaway in EV batteries using hybrid energy storage and phase change materials, *RSC Adv.*, 2025, **15**(31), 24947–24974.
10 Z. Jiang, H. Li and Z. Qu, Recent progress in lithium-ion battery thermal management for a wide range of temperature and abuse conditions, *Int. J. Hydrogen Energy*, 2022, **47**(15), 9428–9459.
11 Y. Zhang, W. Zhang and K. Wenjun, Comparative study on the performance of different thermal management for energy storage lithium battery, *J. Energy Storage*, 2024, **85**, 111028.
12 C. Wu, Y. Sun and T. Heng, A review on the liquid cooling thermal management system of lithium-ion batteries, *Appl. Energy*, 2024, **375**, 124173.
13 C. Liu, X. Dengji and W. Jingwen, Phase Change Materials Application in Battery Thermal Management System: A Review, *Materials*, 2020, **13**, 4622.
14 Q. Gu, L. Guijing and W. Zhaoran, The analysis on the battery thermal management system with composite phase change materials coupled air cooling and fins, *J. Energy Storage*, 2022, **56**, 105977.
15 S. Chen, C. Wan and Y. Wang, Thermal analysis of lithium-ion batteries, *J. Power Sources*, 2005, **140**(1), 111–124.
16 N. Ashkan and F. Siamak, Heat generation in lithium-ion batteries with different nominal capacities and chemistries, *Appl. Therm. Eng.*, 2017, **125**, 1501–1517.
17 C. Heubner, M. Schneider and C. Lämmel, Local heat generation in a single stack lithium ion battery cell, *Electrochim. Acta*, 2015, **186**, 404–412.
18 G. Liu, M. Ouyang and L. Lu, Analysis of the heat generation of lithium-ion battery during charging and discharging considering different influencing factors, *J. Therm. Anal. Calorim.*, 2014, **116**(2), 1001–1010.
19 J. Esmaeili and H. Jannesari, Developing heat source term including heat generation at rest condition for Lithium-ion battery pack by up scaling information from cell scale, *Energy Convers. Manage.*, 2017, **139**, 194–205.

© 2026 The Author(s). Published by the Royal Society of Chemistry

Open Access Article. Published on 12 January 2026. Downloaded on 4/4/2026 5:57:19 AM. This article is licensed under a Creative Commons Attribution-NonCommercial 3.0 Unported Licence.

20 G. Guo, L. Bo and B. Cheng, Three-dimensional thermal finite element modeling of lithium-ion battery in thermal abuse application, *J. Power Sources*, 2010, **195**(8), 2393–2398.
21 Y. Fan, B. Yun and L. Chen, Experimental study on the thermal management performance of air cooling for high energy density cylindrical lithium-ion batteries, *Appl. Therm. Eng.*, 2019, **155**, 96–109.
22 G. Sahin, Analytical and numerical investigations on optimal cell spacing for air-cooled energy storage systems, *Int. J. Therm. Sci.*, 2023, **191**, 108332.
23 W. Meiwei, S. Teng and H. Xi, Cooling performance optimization of air-cooled battery thermal management system, *Appl. Therm. Eng.*, 2021, **195**, 117242.
24 M. Wu, Multi-objective optimization of U-type air-cooled thermal management system for enhanced cooling behavior of lithium-ion battery pack, *J. Energy Storage*, 2022, **56**, 106004.
25 L. Luo, L. Yicai and L. Zimiao, Optimal structure design and heat transfer characteristic analysis of X-type air-cooled battery thermal management system, *J. Energy Storage*, 2023, **67**, 107681.
26 S. Xueyang, C. Tianao and H. Chunmin, Thermal analysis of modified Z-shaped air-cooled battery thermal management system for electric vehicles, *J. Energy Storage*, 2023, **58**, 106356.
27 X. Song, W. Tao and Z. Fanglin, Numerical Simulation and Optimal Design of Air Cooling Heat Dissipation of Lithium-ion Battery Energy Storage Cabin, *J. Phys.: Conf. Ser.*, 2022, **2166**, 012023.
28 A. Mohsen, T. Kalogiannis and J. Jaguemont, A comparative study between air cooling and liquid cooling thermal management systems for a high-energy lithium-ion battery module, *Appl. Therm. Eng.*, 2021, **198**, 117503.
29 A. Pourya, Y. Amin and H. Ehsan, Design improvement of thermal management for Li-ion battery energy storage systems, *Sustain. Energy Technol. Assess.*, 2021, **44**, 101094.
30 A. Ahmed, N. Sameer Mahmoud and H. Jaffal, Numerical and experimental investigation of heat transfer in liquid cooling serpentine mini-channel heat sink with different new configuration models, *Therm. Sci. Eng. Prog.*, 2018, **6**, 128–139.
31 Y. Jin, R. Sun and Z. He, Research on the Heat Dissipation of Lithium-Ion Battery Packs Based on a New Composite Flow Channel Cold Plate, Sichuan Provincial Society of Automotive Engineering, Chengdu Society of Automotive Engineering, *Proceedings of the 17th Sichuan Provincial Automotive Industry Academic Annual Conference*, School of Automotive and Transportation, Xihua University; Sichuan Provincial Key Laboratory of Measurement and Control Technology, 2023, p. 9.
32 S. Gao, Z. Jianyong and L. Yun, Multi-Parameter Optimization and Performance Analysis of Liquid Cooling Plate, *Shandong Ind. Tech.*, 2018, **06**, 133–134.
33 Y. Jianwu, C. Yaling and F. Guanghui, Structural Design and Heat Dissipation Performance Analysis of Parallel Flow Channel Liquid Cooling Plates for Lithium Batteries, *J. Jilin. Univ.*, 2022, **52**(12), 2788–2795.
34 D. Tao, Z. Guodong and R. Yan, Study on thermal management of rectangular Li-ion battery with serpentine-channel cold plate, *Int. J. Heat Mass Transfer*, 2018, **125**, 143–152.
35 W. Ningbo, L. Congbo and L. Wei, Heat dissipation optimization for a serpentine liquid cooling battery thermal management system: An application of surrogate assisted approach, *J. Energy Storage*, 2021, **40**, 102771.
36 H. Shuntao, L. Xinli and L. Yifei, Heat Dissipation Simulation and Optimization of Serpentine Channel Liquid-Cooled Battery Thermal Management System, *Power Technol.*, 2023, **47**(11), 1414–1418.
37 G. Rong and L. Lu, Heat dissipation analysis and optimization of lithium-ion batteries with a novel parallel-spiral serpentine channel liquid cooling plate, *Int. J. Heat Mass Transfer*, 2022, **189**, 122706.
38 L. Fan, L. Jingxue and C. Ya, Study on the cooling performance of a new secondary flow serpentine liquid cooling plate used for lithium battery thermal management, *Int. J. Heat Mass Transfer*, 2024, **218**, 124711.
39 L. Haoxuan, C. Long and Z. Hongyan, Performance enhancement of a battery thermal management system using novel liquid cold plates with micro-channel featuring pin fins, *Energy*, 2024, **301**, 131731.
40 L. Huaqiang, G. Xiangcheng and Z. Jiyun, Liquid-based battery thermal management system performance improvement with intersected serpentine channels, *Renewable Energy*, 2022, **199**, 640–652.
41 Z. Rao and X. Zhang, Investigation on thermal management performance of wedge-shaped microchannels for rectangular Li-ion batteries, *Int. J. Energy Res.*, 2019, **43**, 3876–3890.
42 L. Xue, Z. Furen and L. Xinglong, Performance Optimization of Serpentine Channel Liquid Cooling Plates for Lithium-Ion Power Batteries, *J. Automot. Saf. Energy.*, 2023, **14**(03), 385–392.
43 W. Tang, H. Ding and X. Xiaoming, Research on battery liquid-cooled system based on the parallel connection of cold plates, *J. Renew. Sustain. Energy.*, 2020, **12**(4), 045701.
44 Y. Chen, L. Fan and L. Jingxue, Heat Dissipation Performance of Lithium-Ion Batteries with Secondary Flow Serpentine Channels, *Energy Storage Sci. Technol.*, 2023, **12**(06), 1880–1889.
45 Y. Yi, L. Wenchao and X. Xiaoming, Heat dissipation analysis of different flow path for parallel liquid cooling battery thermal management system, *Int. J. Energy Res.*, 2020, **44**(1), 1–12.
46 L. Rui and W. Tie, Battery Thermal Simulation and Optimization Based on Bidirectional Parallel Flow Channel Liquid Cooling Plates, *Vehicle and Power Tech.*, 2023, (02), 14–19.
47 Y. Chen, K. Chen and Y. Dong, Bidirectional symmetrical parallel mini-channel cold plate for energy efficient cooling of large battery packs, *Energy*, 2022, **242**, 122553.

Open Access Article. Published on 12 January 2026. Downloaded on 4/4/2026 5:57:19 AM. This article is licensed under a Creative Commons Attribution-NonCommercial 3.0 Unported Licence.

48 K. Chen, Y. Chen and S. Mengxuan, Multi-parameter structure design of parallel mini-channel cold plate for battery thermal management, *Int. J. Energy Res.*, 2020, **44**(5), 4321–4334.
49 H. Ren, Li Jia and D. Chao, Experimental Investigation on Pouch Lithium-ion Battery Thermal Management with Mini-Channels Cooling Plate Based on Heat Generation Characteristic, *J. Therm. Sci.*, 2022, **31**(5), 816–829.
50 H. Ren, Y. Liaofei and D. Chao, Phase-change cooling of lithium-ion battery using parallel mini-channels cold plate with varying flow rate, *Case Stud. Therm. Eng.*, 2023, **45**, 102960.
51 Z. Ding, L. Zhiguo and A. Chao, Research on battery thermal management system based on liquid cooling plate with honeycomb-like flow channel, *Appl. Therm. Eng.*, 2023, **218**, 119324.
52 W. Jianfeng, L. Xiaodong and L. Fen, Numerical optimization of the cooling effect of the bionic spider-web channel cold plate on a pouch lithium-ion battery, *Case Stud. Therm. Eng.*, 2021, **26**, 101124.
53 F. Zhang, H. Zhikai and L. Shiyuan, Design and thermal performance analysis of a new micro-fin liquid cooling plate based on liquid cooling channel finning and bionic limulus-like fins, *Appl. Therm. Eng.*, 2024, **237**, 121597.
54 L. Bo, W. Wenhao and B. Shaoyi, Analysis of Heat Dissipation Performance of Battery Liquid Cooling Plate Based on Bionic Structure, *Sustainability*, 2022, **14**, 5541.
55 Y. Zhou, Z. Wang and X. zongfa, Parametric Investigation on the Performance of a Battery Thermal Management System with Immersion Cooling, *Energies*, 2022, **15**, 2554.
56 J. Han, G. Kunalsandip and H. seongguk, Experimental Study on Dielectric Fluid Immersion Cooling for Thermal Management of Lithium-Ion Battery, *Symmetry*, 2022, **14**, 2126.
57 J. Zhu, Y. Zhuang and H. Ouyang, Progress in the Application of Immersed Liquid Cooling Technology in Thermal Management of Power Batteries, *Chin. J. Refrig.*, 2024, **08**, 1–18.
58 K. Jithin and P. Rajesh, Numerical analysis of single-phase liquid immersion cooling for lithium-ion battery thermal management using different dielectric fluids, *Int. J. Heat Mass Transfer*, 2022, **188**, 122608.
59 N. Ahmad Restian Adi, I. Pranoto and H. Mukhtar Ariyadi, Experimental Study on Single-Phase Immersion Cooling for Thermal Management of Lithium-Ion Battery, *International Conference on Engineering, Construction, Renewable Energy, and Advanced Materials*, 2024.
60 S. Hemavathi, A. Thiru Kumaran and S. Srinivas, Synthetic ester-based forced flow immersion cooling technique for fast discharging lithium-ion battery packs, *J. Energy Storage*, 2024, **97**, 112852.
61 Z. Wang, Z. Zhang and S. Lei, Simulation Study on Immersed Thermal Management Performance of Lithium-Ion Batteries, *Cryog. Supercond.*, 2023, **51**(12), 64–72.
62 L. Jiahao, M. Qingwen and L. Xianbin, Numerical study on heat dissipation performance of a lithium-ion battery module based on immersion cooling, *J. Energy Storage*, 2023, **66**, 107511.
63 L. Qian, S. Qianlei and L. Kaixuan, Immersed Cooling Thermal Management of Lithium-Ion Batteries Combined with Checkerboard Topology Split Flow Structure, *Power Generation Tech.*, 2021, **42**(02), 218–229.
64 C. Hongseok, L. Hyoseong and K. Jeebeom, Hybrid single-phase immersion cooling structure for battery thermal management under fast-charging conditions, *Energy Convers. Manage.*, 2023, **287**, 117053.
65 H. Zhu, M. Yinjie and E. Jiaqiang, Channel structure design and optimization for immersion cooling system of lithium-ion batteries, *J. Energy Storage*, 2024, **77**, 109930.
66 H. Hai, L. Wei and X. Shusheng, Single-phase static immersion-cooled battery thermal management system with finned heat pipes, *Appl. Therm. Eng.*, 2024, **254**, 123931.
67 P. Suresh, S. Jaehyeong and L. Mooyeon, A novel dielectric fluid immersion cooling technology for Li-ion battery thermal management, *Energy Convers. Manage.*, 2021, **229**, 113715.
68 W. Yuhang, L. I. Chaoen and W. Xiaodong, Experimental studies on two-phase immersion liquid cooling for Li-ion battery thermal management, *J. Energy Storage*, 2023, **72**, 108748.
69 L. Chaoen, W. Yuhang and S. Zhiwei, Two-phase immersion liquid cooling system for 4680 Li-ion battery thermal management, *J. Energy Storage*, 2024, **97**, 112952.
70 W. Yanfeng, L. Bo and H. Yuli, Experimental study on immersion phase change cooling of lithium-ion batteries based on R1233ZD(E)/ethanol mixed refrigerant, *Appl. Therm. Eng.*, 2023, **220**, 119649.
71 N. P. Williams, D. Trimble and S. M. O'shaughnessy, Liquid immersion thermal management of lithium-ion batteries for electric vehicles: An experimental study, *J. Energy Storage*, 2023, **72**, 108636.
72 G. Luca, D. Valerio and F. Matteo, Experimental study of a direct immersion liquid cooling of a Li-ion battery for electric vehicles applications, *Int. J. Heat Technol.*, 2022, **40**(1), 1–8.
73 X. Lin, Z. Zhou and Y. Jing, A comparative investigation of two-phase immersion thermal management system for lithium-ion battery pack, *J. Clean. Prod.*, 2024, **434**, 140472.
74 C. Wu and C. Liang, Experimental Study on Lithium-Ion Batteries Based on Immersed Cooling, *Power Technol.*, 2023, **47**(11), 1409–1413.
75 L. Yuefeng, X. Weipan and W. Yintao, Heat Dissipation Design and Thermal Simulation Analysis of an Immersed Liquid Cooling System for Energy Storage Lithium Battery Packs, *Energy Storage Sci. Technol.*, 2024, **06**, 1–12.
76 G. Zhechen, X. Jun and W. Xingzao, Optimized Design of Flat Plate Heat Pipe/Liquid-Cooled Battery Thermal Management System Based on One-Dimensional/Three-Dimensional Thermal Models, *J. Mech. Eng.*, 2023, **59**(22), 79–88.
77 L. Yuan, H. Guo and F. QI, Investigation on liquid cold plate thermal management system with heat pipes for $LiFePO_4$

 © 2026 The Author(s). Published by the Royal Society of Chemistry

Open Access Article. Published on 12 January 2026. Downloaded on 4/4/2026 5:57:19 AM. This article is licensed under a Creative Commons Attribution-NonCommercial 3.0 Unported Licence.

battery pack in electric vehicles, *Appl. Therm. Eng.*, 2021, **185**, 116382.
78 M. Hussein, L. Yossapong and W. Somchai, Experimental study on the thermal performance of a battery thermal management system using heat pipes, *Case Stud. Therm. Eng.*, 2021, **26**, 101029.
79 B. Hamidreza, D. Karimi and B. Mohammadreza, Thermal management analysis using heat pipe in the high current discharging of lithium-ion battery in electric vehicles, *J. Energy Storage*, 2020, **32**, 101893.
80 B. Hamidreza, B. Mohammadreza and K. Danial, Heat pipe air-cooled thermal management system for lithium-ion batteries: High power applications, *Appl. Therm. Eng.*, 2021, **183**, 116240.
81 Y. Yonghuang, S. Huat and S. Yixiang, Numerical analyses on optimizing a heat pipe thermal management system for lithium-ion batteries during fast charging, *Appl. Therm. Eng.*, 2015, **86**, 281–291.
82 L. Jialin, G. Yunhua and L. Yong, Thermal and electrochemical performance of a serially connected battery module using a heat pipe-based thermal management system under different coolant temperatures, *Energy*, 2019, **189**, 116233.
83 W. Yueqi, D. Dan and X. Yi, Study on the Influence of Flat Heat Pipe Structural Parameters in Battery Thermal Management System, *Front. Energy Res.*, 2022, **9**, 797664.
84 J. Dong Soo, Y. Sungho and H. Ho, Performance characteristics of a novel heat pipe-assisted liquid cooling system for the thermal management of lithium-ion batteries, *Energy Convers. Manage.*, 2022, **251**, 115001.
85 M. Lei, Z. Jin and Y. Qi, Study on Thermal Management Performance of Power Batteries Assisted by Liquid-Cooled Heat Pipes, *Cryog. Supercond.*, 2023, **51**(06), 90–96.
86 Q. Zhang, H. Yutao and R. Zhonghao, Numerical study on solid–liquid phase change in paraffin as phase change material for battery thermal management, *Sci. Bull.*, 2016, **61**(5), 391–400.
87 Y. Wang, Z. Wang and M. Haitao, Performance investigation of a passive battery thermal management system applied with phase change material, *J. Energy Storage*, 2021, **35**, 102279.
88 Y. Shan, Z. Maoyong and Z. Lingling, Polyethylene Glycol-Based Phase Change Materials for Battery Thermal Management, *Battery*, 2024, **54**(3), 325–329.
89 Z. Lingling, Z. Maoyong and Y. Shan, Hydrated Salt Phase Change Materials for Thermal Management of Lithium-Ion Batteries, *Battery*, 2024, **54**(2), 217–221.
90 Y. Guohua, Z. Guoqing and J. Liqin, Temperature control of battery modules through composite phase change materials with dual operating temperature regions, *Chem.–Eng. J.*, 2022, **449**, 137733.
91 Y. Zhang, L. Jianli and W. Lizhi, Analysis of Key Issues in Phase Change Temperature Control Materials for Power Batteries, *Chem. Renewable Mater.*, 2022, **50**(02), 258–264.
92 G. Yinliang, L. Jianli and Z. Yunfang, Simulation Study on the Effectiveness of Flexible Composite Phase Change Materials for Thermal Management of Lithium-Ion Batteries, *Chem. Renewable Mater.*, 2024, **52**(03), 187–192.
93 X. Liu, C. Wang and W. Tingting, A novel stable and flexible composite phase change materials for battery thermal management, *Appl. Therm. Eng.*, 2022, **212**, 118510.
94 D. Songjiang, F. Jiao and H. Yongqing, Analysis of Heat Transfer Characteristics of Dual-Gradient Structure Filled Phase Change Materials, *Cryog. Supercond.*, 2023, **51**(01), 52–60.
95 Y. Rekabra, H. Sazzad and H. Jiacheng, Novel design optimization for passive cooling PCM assisted battery thermal management system in electric vehicles, *Case Stud. Therm. Eng.*, 2022, **32**, 101896.
96 F. Liu, W. Jianfeng and L. Yiqun, Performance analysis of phase-change material in battery thermal management with bionic leaf vein structure, *Appl. Therm. Eng.*, 2022, **210**, 118311.
97 A. Shakeel, L. Yanhui and K. Ali, Hybrid battery thermal management by coupling fin intensified phase change material with air cooling, *J. Energy Storage*, 2023, **64**, 107167.
98 H. Zhou, W. Li and W. Yang, A hybrid battery thermal management strategy that couples internal PCM with external air-jet cooling, *J. Energy Storage*, 2024, **98**, 113127.
99 Y. Zhang, Q. Fu and Y. Liu, Investigations of lithium-ion battery thermal management system with hybrid PCM/liquid cooling plate, *Processes*, 2022, **11**(1), 57.
100 H. Chen, G. Wei and L. Xu, Performance study on a novel hybrid thermal management system for cylindrical lithium-ion battery pack based on liquid cooling and PCM, *Appl. Therm. Eng.*, 2025, **271**, 126392.
101 G. Liao, K. Jiang and Z. Feng, Thermal performance of battery thermal management system coupled with phase change material and thermoelectric elements, *J. Energy Storage*, 2021, **43**, 103217.
102 X. Liu, L. Yao and C. Su, A hybrid battery thermal management system coupling with PCM and optimized thermoelectric cooling for high-rate discharge condition, *Case Stud. Therm. Eng.*, 2023, **49**, 103269.
103 I. Sadegh, G. Ayat and S. Soheil, PCM/metal foam and microchannels hybrid thermal management system for cooling of Li-ion battery, *J. Energy Storage*, 2023, **72**, 108789.
104 H. Ren, C. Dang and L. Yin, Optimization research on battery thermal management system based on PCM and mini-channel cooling plates, *Case Stud. Therm. Eng.*, 2024, **53**, 103880.
105 C. Bi, R. Song and L. Yunjun, Simulation Analysis of Battery Thermal Management Based on Microchannel Flat Tube Composite Cooling, *Power Technol.*, 2022, **46**(04), 412–415.
106 Y. Chen, Z. Yijie and F. Jingchun, Numerical investigation on flow and heat transfer characteristics in honeycomb-like microchannel heat sink encapsulated with phase change material, *Appl. Therm. Eng.*, 2023, **232**, 121060.
107 J. Cao, F. Jinxin and F. Xiaoming, A delayed cooling system coupling composite phase change material and nano phase change material emulsion, *Appl. Therm. Eng.*, 2021, **191**, 116888.

Open Access Article. Published on 12 January 2026. Downloaded on 4/4/2026 5:57:19 AM.
This article is licensed under a Creative Commons Attribution-NonCommercial 3.0 Unported Licence.

108 G. Zhang, Z. Liu and Z. Wu, Experimental investigation of battery thermal management system based on micro heat pipe array coupled air cooling, *Therm. Sci. Eng. Prog.*, 2025, **60**, 103493.

109 N. Zhang, Z. Wang and B. Zhang, Performance investigation of battery thermal management system based on L-shaped heat pipe coupled cold plate and optimization of controllable liquid cooling, *Eng. Appl. Comput. Fluid Mech.*, 2024, **18**(1), 2370941.

110 C. Zhang, X. Zhan and W. Bin, A Li-Ion Battery Thermal Management System Combining a Heat Pipe and Thermoelectric Cooler, *Energies*, 2020, **13**(4), 841.

111 Q. Yuan, X. Xiaoming and G. Tong, Effect of coupling phase change materials and heat pipe on performance enhancement of Li-ion battery thermal management system, *Int. J. Energy Res.*, 2021, **45**(4), 5399–5411.

112 C. Song, B. Kong and Z. Zeng, Innovative coupled cooling strategy for enhanced battery thermal management: Synergistic optimization of jet impingement and immersion cooling, *Int. J. Heat Mass Transfer*, 2024, **232**, 125963.

113 Z. Zhang, X. Li and S. Peng, Structural Optimization Design of Jet Cooling Device for Lithium Batteries of New Electric Vehicles, *UPB Sci. Bull. Ser. D*, 2025, **87**, 103–120.

114 P. Panmuang, C. Photong and C. Soemphol, Experimental investigation of batteries thermal management system using water cooling and thermoelectric cooling techniques, *Int. J. Power Electron. Drive Syst.*, 2024, **15**(1), 201–212.

115 F. Renlang, P. Huang and T. Ziyi, Experimental and numerical study on the cooling performance of heat pipe assisted composite phase change material-based battery thermal management system, *Energy Convers. Manage.*, 2022, **272**, 116359.

116 B. Hamidreza, D. Karimi and G. Foad Heidari, PCM assisted heat pipe cooling system for the thermal management of an LTO cell for high-current profiles, *Case Stud. Therm. Eng.*, 2021, **25**, 100920.

117 L. Ziyu, Y. Yuan and X. Cao, Heat pipe/phase change material coupled thermal management in Li-ion battery packs: Optimization and energy-saving assessment, *Appl. Therm. Eng.*, 2022, **208**, 118211.

118 Z. Tang, F. Renlang and H. Peifeng, Modeling analysis on the cooling efficiency of composite phase change material-heat pipe coupling system in battery pack, *J. Loss Prev. Process Ind.*, 2022, **78**, 104829.

119 P. Nandy, S. Adjie Fahrizal and A. Bambang, Performance of beeswax phase change material (PCM) and heat pipe as passive battery cooling system for electric vehicles, *Case Stud. Therm. Eng.*, 2020, **21**, 100655.

120 Y. Wang, Y. Wang and T. He, A numerical study on a hybrid battery thermal management system based on PCM and wavy microchannel liquid cooling, *Renewable Energy*, 2024, **235**, 121273.

121 Y. Zhang, Q. Fu and Y. Liu, Investigations of lithium-ion battery thermal management system with hybrid PCM/liquid cooling plate, *Processes*, 2022, **11**(1), 57.

122 F. Liu, Q. Yang and D. Zheng, A novel battery thermal management system with air-liquid coupled cooling based on particle swarm optimization, *Appl. Therm. Eng.*, 2025, **271**, 126391.

© 2026 The Author(s). Published by the Royal Society of Chemistry